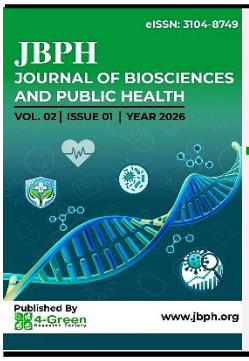

J. Biosci. Public Health 2026; 2(1):68-95

JBPH

Open access

Journal of Biosciences and Public Health

eISSN: 3104-8749

DOI: https://doi.org/10.5455/JBPH.2026.02

Published by: www.4greenresearch.org

Original Research

Genomic and In Silico Characterization of *Acinetobacter* sp. strain HSTU-Asm16 with Plant Growth-Promoting Traits and Diazinon Biodegradation Potential

Sukumar Roy[1,+], Mst. Tahsin Sultana[1,+], Aminur Rahman[2], Md. Shohorab Hossain[3], Bissas Binduraz[1], Tasnim Hanna[1], Md. Amirul Islam Abir[1], Mahbuba Rahman[1], Md. Abdullah-Al-Mamun[4], Monish Kumar Roy[5], Kye Man Cho[6], Md. Azizul Haque[1]*

[+]Both authors have equally contribution to this work

[1]Department of Biochemistry and Molecular Biology, Hajee Mohammad Danesh Science and Technology University, Dinajpur 5200, Bangladesh
[2]Department of Biomedical Sciences, College of Clinical Pharmacy, King Faisal University, Saudi Arabia
[3]Department of Biochemistry and Molecular Biology, Trust University, Barishal, Bangladesh
[4]Yunnan Institute of Parasitic Diseases (YIPD), Chenggong District, Kunming Municipality, Yunnan Province, 650500, P.R. China
[5]Dept. of Chemistry, Dinajpur Govt. College, Dinajpur 5200, Bangladesh
[6]Department of GreenBio Science and Agri-Food Bio Convergence Institute, Gyeongsang National University, Jinju 52727, Republic of Korea

Article information
Received: December 12, 2025
Revised: December 23, 2025
Accepted: December 30, 2025
Published: January 01, 2026

***Corresponding author**
Department of Biochemistry and Molecular Biology, Hajee Mohammad Danesh Science and Technology University, Dinajpur5200, Bangladesh
E-mail: helalbmb2016@hstu.ac.bd
ORCID ID: https://orcid.org/0000- 0002-9788-0766

Keywords: *Acinetobacte*r sp., Endophytic bacteria, plant growth–promoting traits, genomic analysis, organophosphorus hydrolase, Catalytic triads, pesticide biodegradation

Cite this article: Roy S, Sultana MT, Rahman A, Hossain MS, Binduraz B, Hanna T, Abir MAI, Rahman M, Abdullah-Al-Mamun M, Roy MK, Cho KM, Haque MA. Genomic and in silico characterization of *Acinetobacter* sp. strain HSTU-Asm16 with plant growth-promoting traits and diazinon biodegradation potential. J Biosci Public Health. 2026;2(1):68-95. doi:10.5455/JBPH.2026.02

ABSTRACT

Endophytic bacteria with combined plant growth-promoting (PGP) and pesticide biodegradation capacities offer sustainable agroecosystem management. This study reports the isolation, biochemical characterization, whole-genome sequencing, and in silico functional analysis of an endophytic bacterium, *Acinetobacter* sp. strain HSTU-Asm16, isolated from rice (*Oryza sativa* L.). Biochemical assays show catalase, oxidase, and citrate utilization; carbohydrate fermentation; and a suite of extracellular hydrolases consistent with plant-associated metabolism. The draft genome (~3.94 Mb) was annotated using the NCBI PGAP pipeline and analyzed for phylogenetic placement, including phylogenomics, average nucleotide identity (ANI), digital DNA–DNA hybridization (dDDH), pangenome assessment, and synteny analysis. Genome taxonomy placed HSTU-Asm16 within the *Acinetobacter soli* clade, confirming its status as a genomically distinct strain rather than a novel species. The identified genes are used in plant growth promotion (IAA, siderophore biosynthesis, ACC deaminase, and phosphate metabolism), stress tolerance (heat-/cold-shock proteins and heavy-metal resistance), and a complement of putative organophosphate-degrading enzymes (carboxylesterases, phosphotriesterases, amidohydrolases, and opd-like sequences). The genome encodes nif-associated and isc-related iron-sulfur cluster assembly genes, including *nifS*, *nifU*, *iscU*, and *iscA*, are involved in Fe–S protein maturation rather than canonical nitrogen fixation. Molecular docking with representative organophosphate ligands showed plausible substrate active site interactions for several hydrolases. The biochemical, genomic, and in silico evidence indicates *Acinetobacter* sp. HSTU-Asm16 is a promising plant-associated bacterium with dual potential for plant growth promotion and organophosphate pesticide bioremediation in rice farming.

1. INTRODUCTION

Pesticide contamination has become a critical environmental and public health concern worldwide, driven by the extensive and often indiscriminate use of agrochemicals in modern agriculture. Persistent pesticide residues accumulate in soil, water, and food chains, posing serious ecological risks and long-term health hazards to both humans and wildlife [1, 2]. These challenges underscore the urgent need for sustainable and efficient remediation strategies capable of detoxifying contaminated agricultural environments. Among the emerging solutions, microbial bioremediation-particularly using plant-associated bacteria offers a promising, eco-friendly alternative for degrading hazardous agrochemical residues.

Endophytic bacteria, which inhabit the internal tissues of plants without causing harm, have attracted considerable attention for their unique capacity to degrade a wide variety of organic pollutants, including pesticides, within both plant hosts and the surrounding rhizosphere [3, 4]. Their intimate association with plants allows them to complement phytoremediation by enhancing nutrient acquisition, producing growth-promoting hormones, and secreting enzymes that play central roles in the degradation and transformation of xenobiotics. These beneficial traits collectively contribute to improved plant vigor and more efficient removal of contaminants from the environment.

Within the diverse community of endophytes, *Acinetobacter* species have emerged as particularly significant contributors to pesticide bioremediation. Several Acinetobacter strains have been reported to degrade organophosphorus pesticides such as chlorpyrifos, diazinon, and acetamiprid, often functioning as key members of microbial consortia involved in pollutant breakdown [5-7]. Their enzymatic repertoire includes esterases, organophosphorus hydrolases, amidohydrolases, carboxylesterases, and phosphotriesterases, which catalyze the detoxification of diverse pesticide molecules. Notably, enzymes such as molinate hydrolase from *Gulosibacter molinativorax* illustrate the specificity and efficiency with which microbial enzymes can degrade thiocarbamate herbicides [8], demonstrating the broader catalytic potential of pesticide-degrading bacteria.

Beyond their biodegradation abilities, *Acinetobacter* species also contribute significantly to plant growth promotion and nutrient cycling. Some strains, such as *Acinetobacter guillouiae*, demonstrate nitrogen-fixing capabilities that enhance crop growth when used as co-inoculants [9]. Others play key roles in biological nitrogen fixation in crops like sugarcane [10]. Although nitrogen fixation genes such as *nifA* may be present in some genomes, the complete nitrogenase gene cluster is not universal among all strains [11]. Nonetheless, several *Acinetobacter* species including *Acinetobacter sp.* Y16, *A. junii*, and *A. kyonggiensis* are known for heterotrophic nitrification and aerobic denitrification, contributing to nitrogen removal even under low temperatures [12-15]. Phosphate solubilization is another key plant growth-promoting trait widely observed among *Acinetobacter* species. Strains such as *Acinetobacter calcoaceticus*, *A. pittii* gp-1, and *Acinetobacter sp.* RSC7 can transform insoluble phosphorus into bioavailable forms, thereby supporting nutrient uptake in plants [16-18]. Some isolates, including those from karst rocky desertification areas, demonstrate sustained solubilization efficiency under nutrient-limited conditions [19]. Additionally, the ability of *Acinetobacter* species to store polyphosphate [20] supports their metabolic versatility and environmental adaptability. *Acinetobacter* sp. endophytes also influence plant growth through the production of phytohormones such as indole-3-acetic acid (IAA), with strains like *Acinetobacter sp.* PUCM1007 and *A. baumannii* PUCM1029 producing significant levels of this hormone [16]. Siderophore production, another hallmark of *Acinetobacter*

species, enhances iron acquisition and can suppress phytopathogens. Siderophores such as acinetobactin and fimsbactin not only support microbial survival but also promote plant health by limiting pathogen access to iron [21, 22]. Although direct evidence for ACC-deaminase activity in *Acinetobacter* remains limited, these species are well-documented contributors to plant stress tolerance, as shown in *Acinetobacter johnsonii* enhancing resilience in *Populus deltoides* under adverse conditions [23]. In recent years, *in silico* approaches have become indispensable for elucidating the mechanisms underlying microbial pesticide degradation. Virtual screening, molecular docking, molecular dynamics simulations, and homology modeling allow researchers to investigate enzyme–substrate interactions, predict catalytic sites, and assess protein efficiency at a molecular level [24-27].

Considering the previous research outcomes and limitations so far, the present study aims to investigate the bioremediation and plant growth-promoting potential of *Acinetobacter* sp. endophytes through integrated microbiological and computational approaches. By combining genomic, biochemical, and in silico analyses, this research seeks to advance the development of sustainable microbial solutions for pesticide detoxification and improved crop productivity.

2. MATERIALS AND METHODS

2.1. Isolation and biochemical characterization

Endophytic *Acinetobacter* sp. HSTU-Asm16 was isolated from surface-sterilized leaves of healthy *Oryza sativa* L. using standard isolation procedures described previously [5, 7, 28]. The sterilized tissues were macerated and plated onto minimal salt agar supplemented with 1.0% diazinon to selectively enrich pesticide-tolerant endophytes. Distinct colonies were purified and subjected to biochemical identification following the criteria outlined in *Bergey's Manual of Systematic Bacteriology* (1996), including catalase, oxidase, citrate utilization, urease, and triple sugar iron assays [29]. In addition, hydrolytic capabilities such as cellulase, xylanase, and pectinase production were evaluated based on halo formation around colonies on respective substrate-amended agar media [30].

2.2. Genomic DNA extraction, sequencing, assembly, and annotation of *Acinetobacter* sp. HSTU-Asm16

Genomic DNA of *Acinetobacter* sp. HSTU-Asm16 was extracted using the Promega Genomic DNA Extraction Kit following the manufacturer's instructions. DNA concentration and purity were determined with a Promega spectrophotometer. Whole-genome shotgun sequencing was performed on the Illumina MiniSeq platform using paired-end chemistry. Library preparation from purified DNA employed the Nextera XT Library Preparation Kit according to standard protocols [31]. The quality of raw reads was evaluated with FASTQC version (v0.11.9), followed by adapter removal, quality trimming, and length filtering using the FASTQ Toolkit and assembled *de novo* with SPAdes v3.9.0. Resulting contigs were scaffolded, refined, and genome alignments were generated using Progressive Mauve v2.4.0 [32]. Genome assembly quality was assessed using SPAdes v3.9.0, and assembly metrics including total contigs, N50, genome size, GC content, and coverage were calculated using QUAST v5.2.0.

Genome annotation was conducted using both the NCBI Prokaryotic Genome Annotation Pipeline (PGAP v4.5) [33, 34]. Functional categorization of coding sequences was carried out using the COG database via the RAST annotation server,

complemented by PGAP-derived annotations [35]. Multilocus sequence typing was performed, aligning with established methods for bacterial typing using whole-genome sequencing data [36]. Phylogenetic analyses based on the housekeeping genes *rec*A, *gyr*B, and *rpo*B were performed in MEGA XI with 1,000 bootstrap replicates [29]. Genes associated with nitrogen fixation, phosphate solubilization, phytohormone production, biofilm development, and abiotic stress responses were identified [33, 37, 38].

2.3. Comparative genomic and functional analyses

2.3.1. Phylogenetic and average nucleotide identity analysis

Housekeeping genes, including *rpo*B, *rec*A, and *gyr*B, were extracted from the annotated genome of *Acinetobacter* sp. HSTU-Asm16. Each gene was aligned individually, followed by concatenation for phylogenetic reconstruction. Neighbor-joining trees based on both the 16S rRNA gene and concatenated markers were generated using MEGA X. Whole-genome phylogenetic relationships were inferred using REALPHY 1.12 (http://www.realphy.unibas.ch /realphy/) by incorporating the genome of the target strain alongside its closest relatives. Average nucleotide identity (ANIb) between *Acinetobacter* sp. HSTU-Asm16 and related taxa was calculated using the JSpeciesWS platform (http://jspecies.ribhost.com/jspeciesws) [29, 33]

2.3.2. Digital DNA–DNA hybridization (dDDH)

Genome-level similarity was further assessed via digital DNA–DNA hybridization using the Genome-to-Genome Distance Calculator (GGDC 3.0; https://ggdc.dsmz.de/). dDDH values were determined following standard formulas, comparing the target strain with fourteen phylogenetically related *Acinetobacter* genomes.

2.3.3. Genome alignment and synteny analysis

Whole-genome alignment of *Acinetobacter* sp. HSTU-Asm16 was performed using the MAUVE algorithm to visualize syntenic regions and structural variations. Colored blocks representing synteny facilitated the comparison of genomic architecture. Pangenome analysis was conducted using publicly available servers as described by [5] to examine gene distribution patterns across related species.

2.3.4. Genome-level comparison

To investigate genomic features, the draft genome of *Acinetobacter* sp. HSTU-Asm16 was compared with recently reported, closely related genomes. Circular and linear genome maps were generated using CGView (http://www.cgview) and BRIG v0.95, respectively. Sequence similarity was assessed via BLAST+ with identity thresholds of 70–90% and an E-value cutoff of 10. Genome collinearity and synteny were further examined using Progressive Mauve (http://darlinglab.org/mauve/mauve.html). Additionally, in-silico DNA–DNA hybridization was performed with the fifteen nearest genomes using the GGDC server.

2.4. Functional Gene Annotation: Plant growth promotion, stress tolerance, and insecticide degradation

Genes associated with plant growth–promoting (PGP) traits were mined from PGAP-annotated genome assemblies and compared with genomes of representative endophytic reference strains. Key functional categories identified included nitrogen metabolism–related genes (nifS–nifU and Fe–S cluster assembly genes *iscA, iscU,* and *iscR*, rather than complete *nifA–nifZ* clusters), nitrosative stress response and nitrogen regulation genes (norRV, ntrB, glnK, and nsrR), ammonia assimilation–associated genes, ACC deaminase–related enzymes, siderophore biosynthesis genes associated with enterobactin production, tryptophan-dependent indole-3-acetic acid (IAA) biosynthesis–related genes, and genes involved in phosphate and sulfur metabolism. Additional PGP-associated functional categories included biofilm formation and adhesion, chemotaxis and root colonization, trehalose metabolism, antioxidant defense systems (e.g., superoxide dismutase), diverse hydrolase-encoding genes, and genes linked to symbiosis-related pathways and antimicrobial peptide biosynthesis. Genes associated with abiotic stress tolerance, including cold-shock proteins, heat-shock proteins, drought/osmotic stress–responsive genes, and heavy metal resistance determinants, were also catalogued. Furthermore, genes putatively involved in organophosphate metabolism were identified based on functional annotation and homology to previously reported enzymes, including carboxylesterases, putative organophosphorus hydrolases (*opd*-like), amidohydrolases, phosphonatases, phosphotriesterases, and phosphodiesterases, in accordance with prior literature reports [39, 40].

2.5. Virtual screening and catalytic triad visualization

The 3D structures of the organophosphate insecticides investigated were obtained from the PubChem database (https://pubchem.ncbi.nlm.nih.gov/) and organized for virtual screening. Prior to docking, the ligand molecules were subjected to geometry optimization and energy minimization using the MMFF94 force field with the steepest-descent method. Virtual screening was carried out in PyRx, where each ligand was individually docked with the selected protein targets. Multiple docking simulations were performed per enzyme to assess potential interactions within the active site and to confirm consistent binding patterns. Binding energies (kcal/mol) were extracted and visualized using R software. Enzymes with docking energies stronger than –7 kcal/mol were analyzed further, and detailed visualizations of key catalytic motifs, such as Ser-His-Asp and Ser-His-His triads, were generated to infer possible enzymatic mechanisms for insecticide degradation [24, 29].

2.6. Pesticides degrading protein modeling and docking with pesticides

Candidate pesticide-degrading enzymes were predicted and modeled using SWISS-MODEL and I-TASSER [37]. The structural integrity and reliability of the predicted models were assessed using ERRAT, VERIFY3D, and Ramachandran plot evaluation. Docking simulations conducted through PyRx and Discovery Studio revealed strong ligand–protein interactions, with binding energies ranging between –6.5 and –8.0 kcal·mol^{-1}, and highlighted critical catalytic residues implicated in organophosphorus pesticides degradation [34, 38].

3. RESULTS

3.1. Biochemical characterization of the newly isolated endophytic bacteria

Table 1 depict the biochemical characteristics of the three newly isolated bacterial strain *Acinetobacter* sp. HSTU-Asm16 sourced from rice plants. The strains showed positive reactions for oxidase, citrate utilization, and catalase (**Table 1**). While *Acinetobacter* sp. HSTU-Asm16 showed positive motility for both indole and urease tests. In the Methyl red test, *Acinetobacter* sp. HSTU-Asm16 was positive, conversely, the strains exhibited opposite result patterns in the Voges Proskauer test. Interestingly, the strain showed positive activity for both the TSI test and the carbohydrate (lactose, sucrose, dextrose) utilization test (**Table 1**). Additionally, the strain was negative for the indole test but positive for the urease test. While cell wall hydrolytic enzymes activities, including xylanase, amylase, and protease were found in the strain, but CMCase activity was absent in the *Acinetobacter* sp. HSTU-Asm16 (**Table 1**).

Table 1. Biochemical analyses of *Acinetobacter* sp. HSTU-ASm16.

	Oxidase	Citrate	Catalase	MIU	Mortality	Urease	VP	MR	TSI	Lactose	Sucrose	Dextrose	CMCase	Xylanase	Amylase	Protease
Acinetobacter sp. HSTU-Asm16	+	+	+	-	+	+	-	+	+	+	+	+	-	+	+	+

3.2. Genome organization and coding sequence (CDS) distribution

The complete genome map of *Acinetobacter* sp. HSTU-ASm16 is shown as a circular representation (**Figure 1**), with a total genome size of 3,594,127 bp and a linear topology. Genome annotation identified a dense and evenly distributed set of coding DNA sequences (CDSs) across the chromosome. The outermost rings represent annotated CDSs encoded on the forward and reverse strands**,** illustrated by directional arrows that indicate gene orientation. CDSs are distributed throughout the genome without large gene-poor regions, indicating a compact genomic architecture. Genes annotated as protein-coding sequences constitute the majority of features, with additional tracks representing tRNA and rRNA loci, which are interspersed across the chromosome. Inner rings depict GC content and GC skew variation along the genome. GC content shows moderate fluctuation around the genomic average, while GC skew alternates regularly between positive and negative values, consistent with bidirectional DNA replication from a putative origin toward the terminus. Distinct transitions in GC skew are visible, corresponding to replication-related structural features of the chromosome. The innermost ring displays the genomic coordinate scale, highlighting the relative positions of CDSs and structural features along the chromosome. No large-scale chromosomal rearrangements or extensive low-complexity regions were observed in the assembled genome.

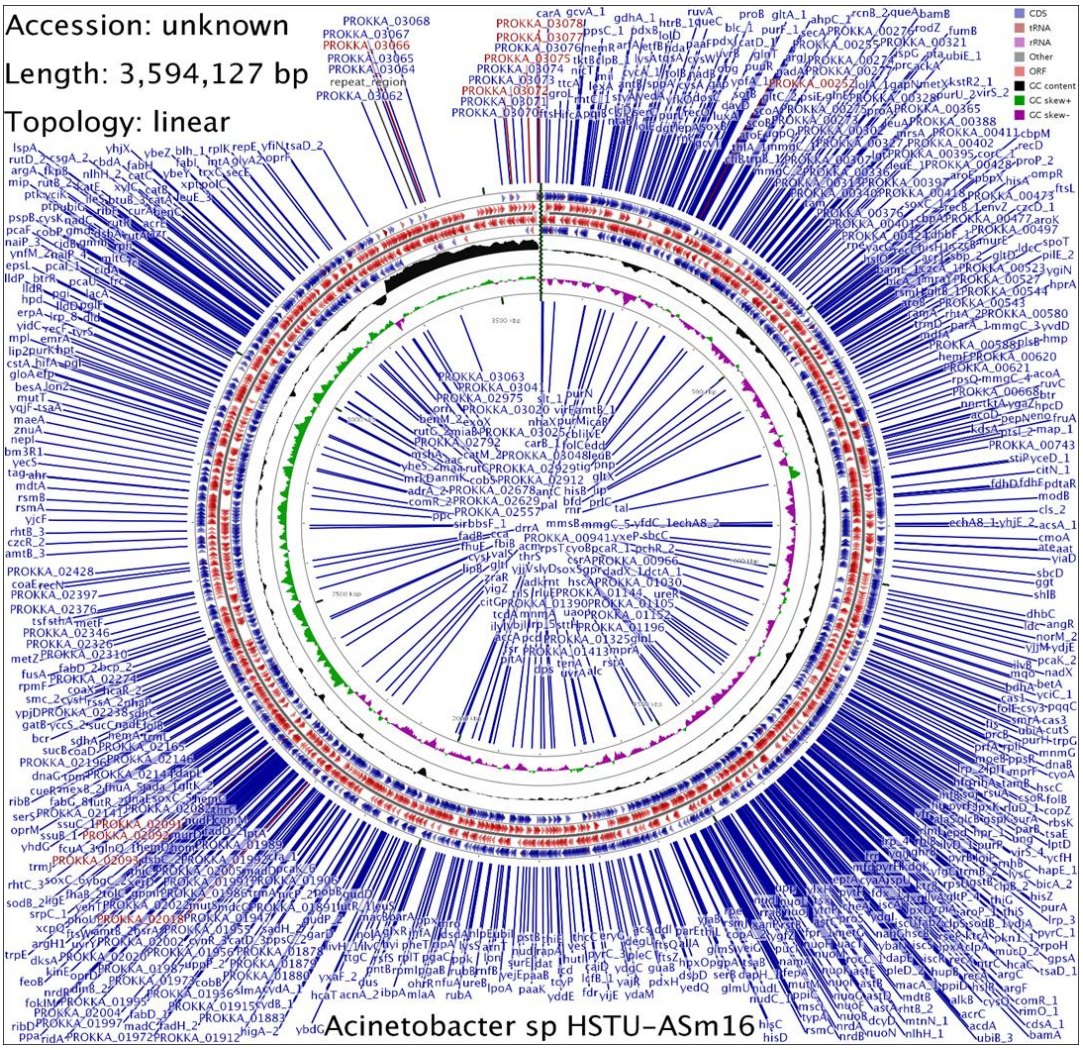

Figure 1. Circular genome map of *Acinetobacter* sp. strain HSTU-Asm16. The draft genome (3,594,127 bp) is shown in circular form. From outer to inner rings: protein-coding sequences on the forward strand (blue) and reverse strand (red), tRNA genes (pink), rRNA genes (purple), followed by GC content (black) and GC skew (green and purple). Selected gene labels illustrate the compact and evenly distributed genomic organization.

3.3. Phylogenetic taxonomy of the endophytic bacteria

3.3.1. Whole genome phylogenetic analysis

A whole-genome based phylogenetic tree was constructed to determine the evolutionary placement of *Acinetobacter* sp. HSTU-ASm16 among representative species of the genus *Acinetobacter* (**Figure 2A**). The analysis included multiple reference genomes from closely related species, including *A. baumannii*, *A. pittii*, *A. calcoaceticus*, *A. nosocomialis*, *A. haemolyticus*, *A. junii*, *A. johnsonii*, *A. lwoffii*, *A. indicus*, and *A. soli*. In the resulting phylogeny, *Acinetobacter* sp. HSTU-ASm16 clustered most closely with *Acinetobacter soli* strain GFJ2, forming a distinct and well-supported lineage separate from other *Acinetobacter* species. This cluster was clearly resolved from the clades comprising clinically relevant *A. baumannii* strains, which grouped together in a separate, well-defined branch.

Additional species-level groupings were observed, including distinct clusters for *A. pittii*, *A. nosocomialis*, *A. calcoaceticus*, *A. haemolyticus*, and *A. johnsonii*, each forming coherent lineages consistent with their taxonomic assignments. *Acinetobacter* sp. HSTU-ASm16 did not cluster within any of these species-specific clades other than *A. soli*. Overall, the whole-genome phylogenetic analysis places *Acinetobacter* sp. HSTU-ASm16 within the *A. soli* related lineage**,** while maintaining clear separation from other closely related *Acinetobacter* species included in the analysis.

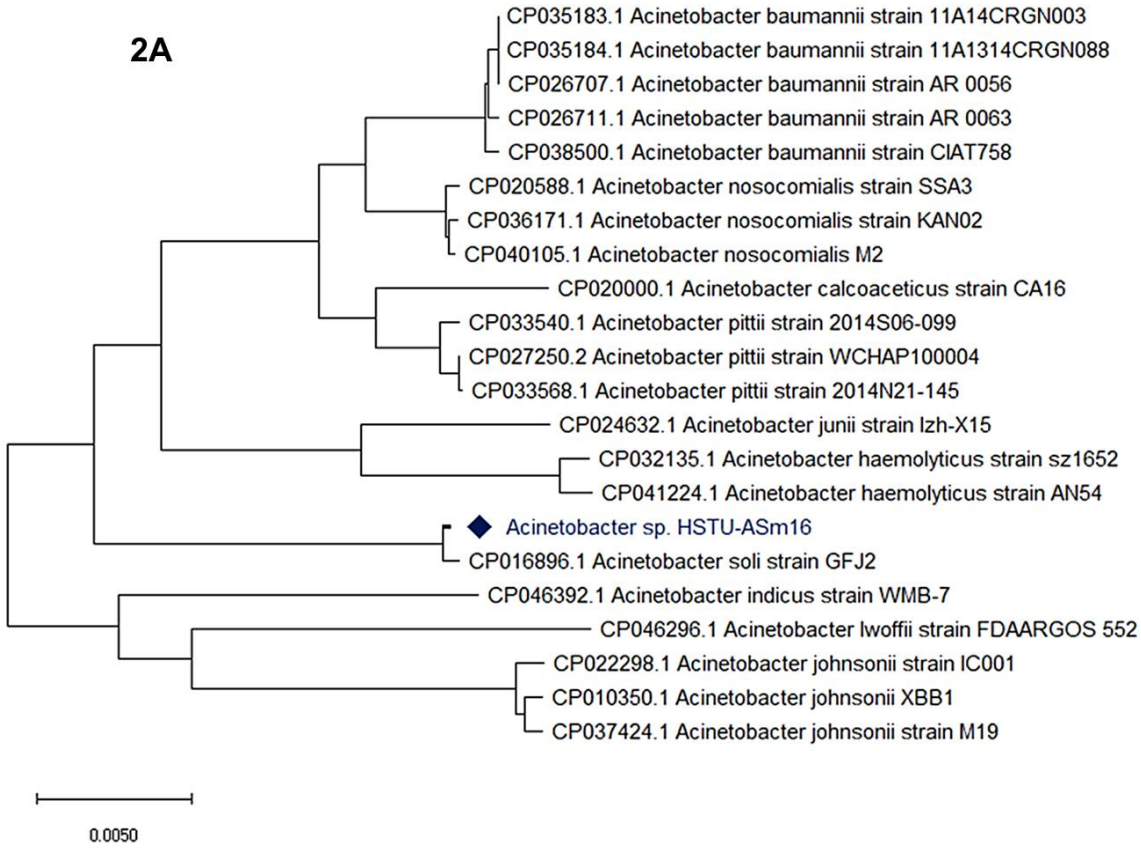

Figure 2. **(A)** Whole genome phylogenetic tree of the strain *Acinetobacter* sp. HSTU-Asm16.

3.3.2. Housekeeping genes phylogeny analysis

The phylogenetic tree based on the *rec*A housekeeping gene was constructed to determine the evolutionary relationship of *Acinetobacter* sp. HSTU-ASm16 with closely related *Acinetobacter* species. The analysis revealed that HSTU-ASm16 clustered closely with *Acinetobacter soli* strain GFJ2, forming a distinct clade with a high bootstrap value of 100, indicating strong phylogenetic relatedness (**Figure 2B**). Other *Acinetobacter* species formed separate, well-supported clusters: *A. baumannii* strains (11A1314CRGN088, CIAT758, 11A14CRGN003, AR 0056, AR 0063) grouped together with a bootstrap value of 100, reflecting close intra-species relationships, while *A. pittii* strains (WCHAP100004 and 2014N21-145) also clustered with 100% bootstrap support. In contrast, *A. calcoaceticus*, *A. haemolyticus*, *A. johnsonii*, and *A. lwoffii* each formed separate branches, highlighting their genetic divergence from the study strain. Overall, the recA-based phylogeny indicates that *Acinetobacter* sp. HSTU-ASm16 is most closely related to *A. soli*, supporting its classification as

a distinct species within the genus.

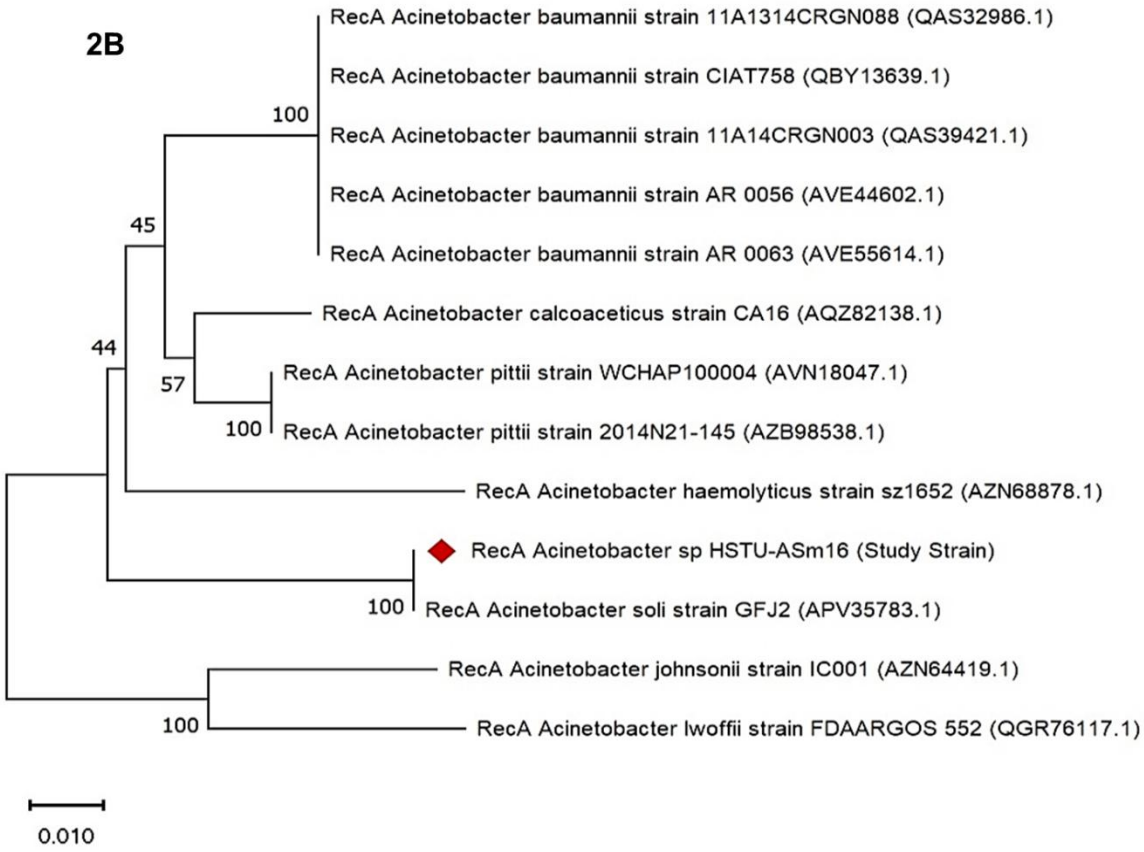

Figure 2B. *rec*A gene phylogenetic tree of the strain *Acinetobacter* sp. HSTU-Asm16.

The phylogenetic tree based on *gyr*B gene sequences revealed the evolutionary relationships among *Acinetobacter* strains. The study strain, *Acinetobacter* sp. HSTU-ASm16, clustered closely with *Acinetobacter soli* strain GFJ2, supported by a bootstrap value of 100 (**Figure 2C)**. Several *Acinetobacter baumannii* strains (11A1314CRGN088, 11A14CRGN003, AR 0056, CIAT758, AR 0063) formed a distinct cluster with bootstrap values ranging from 62 to 100. *Acinetobacter pittii* strain WCHAP100004 formed a separate lineage, while *Acinetobacter haemolyticus* strain sz1652 branched with a bootstrap value of 78.

More distantly related species, including *Acinetobacter lwoffii* strain FDAARGOS 552 and *Acinetobacter johnsonii* strain IC001, were positioned at the base of the tree, indicating early divergence within the genus. Bootstrap values across the tree ranged from 62 to 100, reflecting the statistical support for each clade.

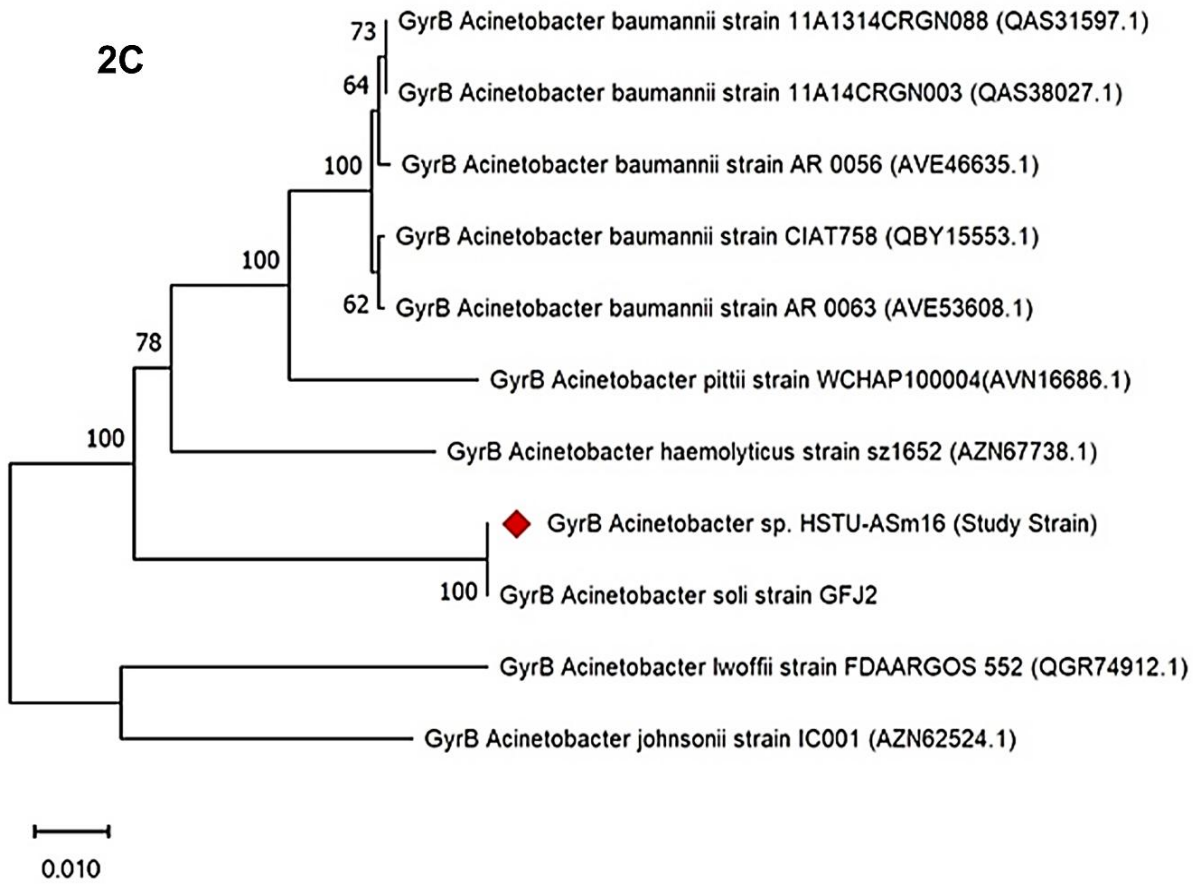

Figure 2C. *gyrB* gene phylogenetic tree of the strain *Acinetobacter* sp. HSTU-Asm16.

The phylogenetic tree based on rpoB gene sequences showed the evolutionary relationships among *Acinetobacter* strains. The study strain, *Acinetobacter* sp. HSTU-ASm16, clustered closely with *Acinetobacter soli* strain GFJ2, supported by a bootstrap value of 100 (**Figure 2D)**. Several *Acinetobacter baumannii* strains (11A1314CRGN088, 11A14CRGN003, AR 0056, AR 0063, CIAT758) formed a distinct cluster with bootstrap values of 89 and 100. *Acinetobacter pittii* strains WCHAP100004 and 2014N21-145 formed a separate clade with a bootstrap value of 100, while *Acinetobacter haemolyticus* strain sz1652 branched off from the main clusters. More distantly related species, including *Acinetobacter lwoffii* strain FDAARGOS 552 and *Acinetobacter johnsonii* strain IC001, formed a basal clade with a bootstrap value of 100. Horizontal branch lengths indicate evolutionary distances, with the scale bar representing 0.0050. Bootstrap values across the tree ranged from 50 to 100, reflecting varying levels of support for the clades.

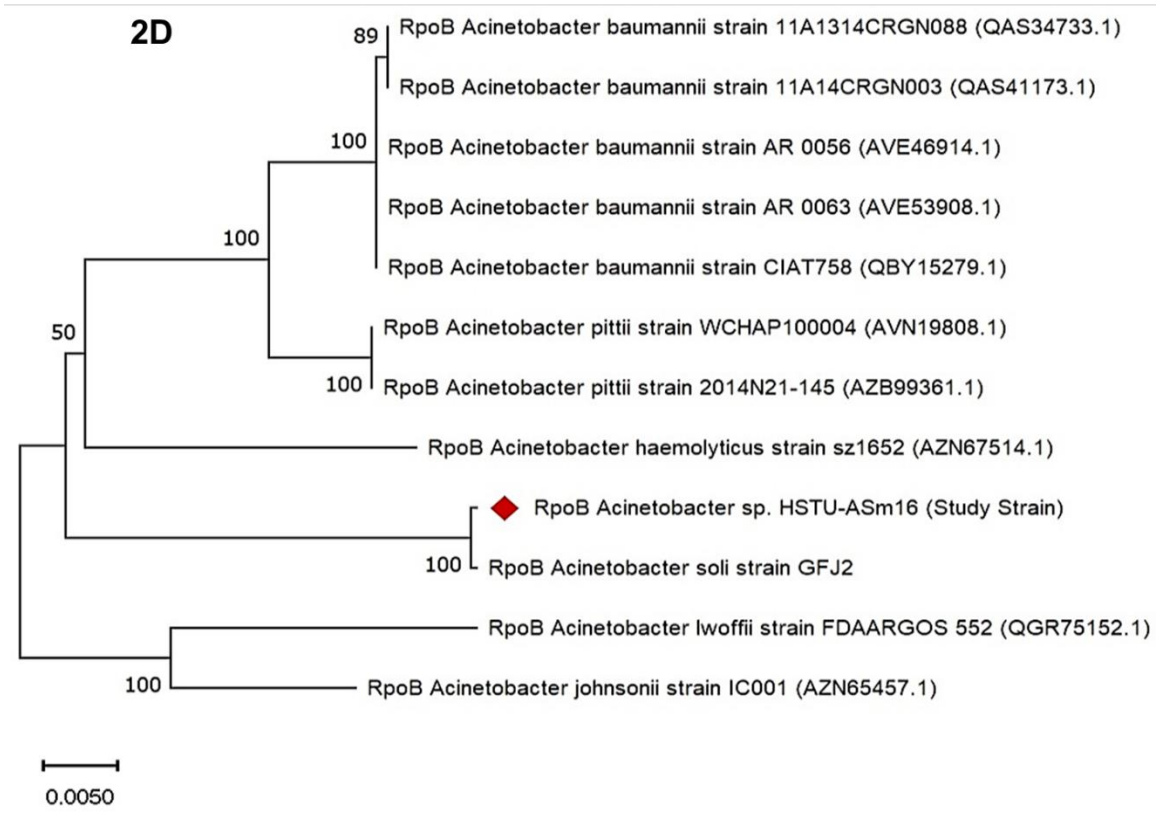

Figure 2D. rpo*B* gene phylogenetic tree of the strain *Acinetobacter* sp. HSTU-Asm16.

3.4. Analyses of the genomes

3.4.1. Average nucleotide identity (ANI) analysis of the strain

Average nucleotide identity (ANI) analysis was conducted using the JSpeciesWS platform to assess the genomic relatedness of *Acinetobacter* sp. HSTU-ASm16 with 14 phylogenetically related *Acinetobacter* reference genomes (**Table 2**). The highest ANI value (98.73%) for *Acinetobacter* sp. HSTU-ASm16 was observed with *Acinetobacter soli* strain GFJ2 (CP016896.1). This value represents the only comparison exceeding 95% ANI**,** indicating the closest genomic relationship among the analyzed taxa. ANI values between HSTU-ASm16 and other *Acinetobacter* species, including *A. baumannii*, *A. pittii*, *A. calcoaceticus*, *A. johnsonii*, *A. haemolyticus*, *A. lwoffii*, and *A. indicus*, ranged from 83.72% to 84.66%**,** well below the commonly accepted species delineation threshold. In contrast, intra-species ANI values among reference *A. baumannii* strains were consistently high, ranging from 97.88% to 99.99%**,** confirming the reliability of the ANI analysis and the resolution of the dataset. Similarly, high ANI values were observed among *A. pittii* strains (up to 99.15%**),** supporting established species boundaries within the genus. Overall, the ANI results demonstrate that *Acinetobacter* sp. HSTU-ASm16 is most closely related to *A. soli* strain GFJ2, while remaining genomically distinct from other examined *Acinetobacter* species**,** including clinically relevant *A. baumannii* strains.

Table 2. Average Nucleotide identity (ANI) of the *Acinetobacter* sp HSTU-ASm16.

	Acinetobacter sp. HSTU-ASm16	CP016896.1 *Acinetobacter soli* strain GFJ2	CP020000.1 *Acinetobacter calcoaceticus* strain CA16	CP022298.1 *Acinetobacter johnsonii* strain IC001	CP026707.1 *Acinetobacter baumannii* strain AR 0056	CP026711.1 *Acinetobacter* baumannii strain AR 0063	CP027250.2 *Acinetobacter pittii* strain WCHAP100004	CP032135.1 Acinetobacter haemolyticus strain sz1652	CP033540.1 Acinetobacter pittii strain 2014S06-099	CP033568.1 *Acinetobacter pittii* strain 2014N21-145	CP035183.1 *Acinetobacter* baumannii strain 11A14CRGN003	CP035184.1 Acinetobacter baumannii strain 11A1314CRGN088	CP038500.1 *Acinetobacter baumannii* strain CIAT758	CP046296.1 *Acinetobacter lwoffii* strain FDAARGOS 552	CP046392.1 *Acinetobacter indicus* strain WMB-7
Acinetobacter sp HSTU-ASm16	*	98.73	84.46	83.80	84.03	84.16	84.14	84.66	84.15	84.07	84.11	84.11	84.11	83.74	83.78
CP016896.1 *Acinetobacter soli* strain GFJ2	98.73	*	84.32	84.14	83.93	84.20	84.85	84.70	84.36	84.19	84.14	84.14	84.13	84.00	84.00
CP020000.1 *Acinetobacter calcoaceticus* strain CA16	84.46	84.19	*	84.30	87.71	87.66	90.25	84.88	90.18	90.14	87.66	87.64	87.66	84.33	83.99
CP022298.1 *Acinetobacter johnsonii* strain IC001	83.82	84.12	84.30	*	84.71	84.28	84.74	84.94	84.44	84.74	84.26	84.27	85.33	85.81	86.23
CP026707.1 *Acinetobacter baumannii* strain AR 0056	84.02	83.99	87.69	84.69	*	98.15	89.13	85.37	89.10	88.99	99.62	99.62	97.88	85.54	85.25
CP026711.1 *Acinetobacter baumannii* strain AR 0063	84.17	84.26	87.66	84.26	98.16	*	89.09	85.03	89.11	88.88	98.21	98.21	97.92	84.66	84.86
CP027250.2 *Acinetobacter pittii* strain WCHAP100004	84.13	84.85	90.26	84.75	89.14	89.08	*	85.42	96.52	99.15	89.13	89.14	89.21	85.34	84.72
CP032135.1 *Acinetobacter haemolyticus* strain sz1652	84.64	84.68	84.89	84.88	85.33	85.00	85.38	*	85.14	85.23	85.10	85.11	85.30	85.50	85.49
CP033540.1 *Acinetobacter pittii* strain 2014S06-099	84.15	84.36	90.18	84.54	89.10	89.11	96.52	85.16	*	96.34	89.11	89.11	89.13	84.90	84.87
CP033568.1 *Acinetobacter pittii* strain 2014N21-145	84.06	84.17	90.16	84.74	88.99	88.88	99.15	85.27	96.34	*	88.88	88.88	89.04	85.63	85.07
CP035183.1 *Acinetobacter baumannii* strain 11A14CRGN003	84.12	84.05	87.66	84.30	99.62	98.20	89.14	85.11	89.11	88.88	*	99.99	97.90	85.23	84.97
CP035184.1 *Acinetobacter baumannii* strain 11A1314CRGN088	84.12	84.05	87.65	84.30	99.62	98.20	89.13	85.12	89.11	88.88	99.99	*	97.91	85.17	84.97
CP038500.1 *Acinetobacter baumannii* strain CIAT758	84.10	84.03	87.68	85.31	97.88	97.93	89.21	85.28	89.13	89.04	97.91	97.91	*	84.90	85.24
CP046296.1 *Acinetobacter lwoffii* strain FDAARGOS 552	83.72	84.01	84.33	85.81	85.54	84.59	85.20	85.58	84.75	85.51	85.16	85.17	84.90	*	85.62
CP046392.1 *Acinetobacter indicus* strain WMB-7	83.78	84.10	83.94	86.20	85.21	84.87	84.71	85.49	84.86	85.09	84.93	84.94	85.23	85.63	*

3.4.2. Digital DNA–DNA hybridization (dDDH) analysis of the strain

Digital DNA–DNA hybridization (dDDH) analysis was performed to further assess the genomic relatedness of *Acinetobacter* sp. HSTU-Asm16 with phylogenetically related *Acinetobacter* reference strains using three recommended formulae (**Table 3**). The highest dDDH values were obtained in comparison with *Acinetobacter soli*, with values of 82.2% (Formula 1), 88.6% (Formula 2), and 86.2% (Formula 3)**.** These values exceed the commonly accepted 70% species delineation threshold**,** indicating a close genomic relationship between HSTU-Asm16 and *A. soli*. The corresponding G+C

content difference (1.86%) was within the range typically observed for strains belonging to the same species. In contrast, dDDH values calculated between *Acinetobacter* sp. HSTU-Asm16 and other reference species including *A. calcoaceticus*, *A. johnsonii*, *A. baumannii*, *A. pittii*, *A. haemolyticus*, *A. lwoffii*, and *A. indicus* were consistently low, ranging from 15.6% to 21.1% across all formulae**.** These values are well below the species-level threshold**,** indicating clear genomic separation from these taxa. Correspondingly, G+C content differences for these comparisons ranged from 0.51% to 6.24%**,** supporting genomic divergence from non-A. *soli* species. Overall, the dDDH results demonstrate that *Acinetobacter* sp. HSTU-Asm16 exhibits species-level genomic relatedness to *A. soli* while remaining distinct from other examined *Acinetobacter* species (**Table 3**).

Table 3. dDDH of the *Acinetobacter* sp. HSTU-Asm16.

Reference strains genome compared	Formula:1 (HSP length / total length) DDH	Formula:2 (identities / HSP length) DDH Recommended	Formula:3 (identities / total length DDH	Difference in % G+C: (interpretation : distinct species)
Acinetobacter soli	82.2	88.6	86.2	1.86
Acinetobacter calcoaceticus strain CA16	17.1	20.2	16.9	6.24
CP022298.1 *Acinetobacter johnsonii* strain IC001	15.9	20.3	15.9	3.48
Acinetobacter baumannii strain AR0056	17.1	20.2	16.8	5.85
Acinetobacter baumannii	17.2	20.4	17	5.97
Acinetobacter pittii strain WCHAP100004	17.2	20.1	17	6.18
Acinetobacter haemolyticus	15.8	21.1	15.8	5.25
Acinetobacter pittii strain 2014S06-099	17	20	16.8	6.15
Acinetobacter pittii strain 2014N21-145	17.1	20	16.9	6.05
Acinetobacter baumannii strain 11A14CRGN003	17	20.3	16.8	5.92
Acinetobacter baumannii strain 11A1314CRGN088	17	20.3	16.8	5.92
Acinetobacter baumannii strain CIAT758	16.9	20.4	16.8	5.95
Acinetobacter lwoffii strain FDAARGOS_552	15.6	20.6	15.6	1.65
Acinetobacter indicus strain WMB-7	16.3	20.1	16.2	0.51

3.4.3. Pangenome analysis of the strain

The comparative genomic analysis of *Acinetobacter* sp. HSTU-ASm16 revealed a dynamic genome architecture characterized by both conserved and variable regions. Alignment with closely related *Acinetobacter* species indicated the presence of large syntenic blocks, suggesting evolutionary conservation of core genomic regions. However, several regions displayed structural variations, including insertions, deletions, and potential inversions, reflecting genome plasticity and strain-specific adaptations.

Notably, genomic islands unique to *Acinetobacter* sp. HSTU-ASm16 were observed, which likely harbor genes associated with specialized metabolic functions, environmental adaptability, and potential plant-associated traits. These regions were absent in some related *Acinetobacter* strains, highlighting strain-specific genomic features. Additionally, evidence of horizontal gene transfer events was inferred from the presence of mobile genetic elements, including transposons and putative plasmid-borne sequences, indicating that HSTU-ASm16 may have acquired novel traits contributing to its ecological versatility. Overall, the genome of *Acinetobacter* sp. HSTU-ASm16 exhibits a combination of conserved syntenic

regions and variable genomic segments, demonstrating both evolutionary conservation and adaptive potential. This genomic organization suggests that HSTU-ASm16 is equipped with genetic elements that may facilitate environmental survival, host interactions, and potentially beneficial plant-associated functions (**Figure 3**).

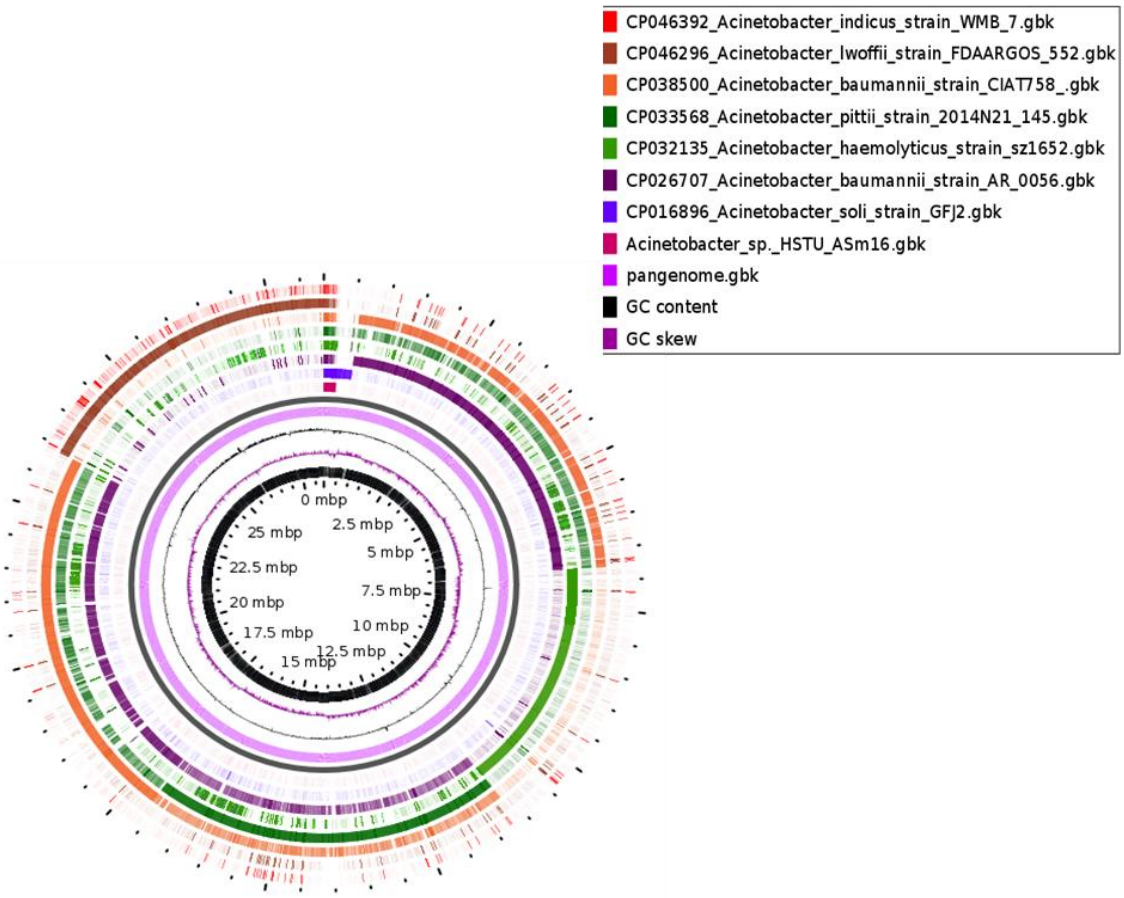

Figure 3. Pangenomic analyses of the strain *Acinetobacter* sp. HSTU-Asm16.

3.4.4. Progressive mauve analysis

Chromosome assemblies of the four samples were reordered according to M63 with Mauve and aligned by using progressive Mauve. The locally collinear blocks (LCB) of the genomes of three nearest strains namely *Acinetobacter baumannii* strain. *Acinetobacter soli* strain TO-A JPC and *Acinetobacter bohemicus* sp. with *Acinetobacter sp.* HSTU-Asm16 strain was inspected using Progressive Mauve (**Figure 4**). The block outlines of *Acinetobacter* sp. HSTU-Asm16 genome encompassed a sort of sequence that is homologous to part of other genomes compared. It is assumed that the homologous LCBs are internally free from genomic rearrangement of genomes compared. In fact, the LCB in the genome of *Acinetobacter* sp. HSTU-A Sm16 is connected by lines to similarly colored LCBs in the genomes of, *Acinetobacter baumannii*, *Acinetobacter soli*, *Acinetobacter bohemicus*, respectively. The boundaries of LCBs of *Acinetobacter* sp. HSTU-Asm16 and other strains taken comparison are generally considered as breakpoints of genome rearrangements. As seen in Figure 4, the LCBs of the *Acinetobacter* sp. HSTU-Asm16 genome are near exactly matched with the LCBs of

genomes taken for comparison. In addition, the reshuffling or rearrangements of sort of sequences are found in various LCBs compared to the LCBs of other nearest strains genomes. These results suggested that the Genome of the *Acinetobacter* sp. HSTU-Asm16 strain is quite varied from its nearest strains, which indicates its evolutionary properties.

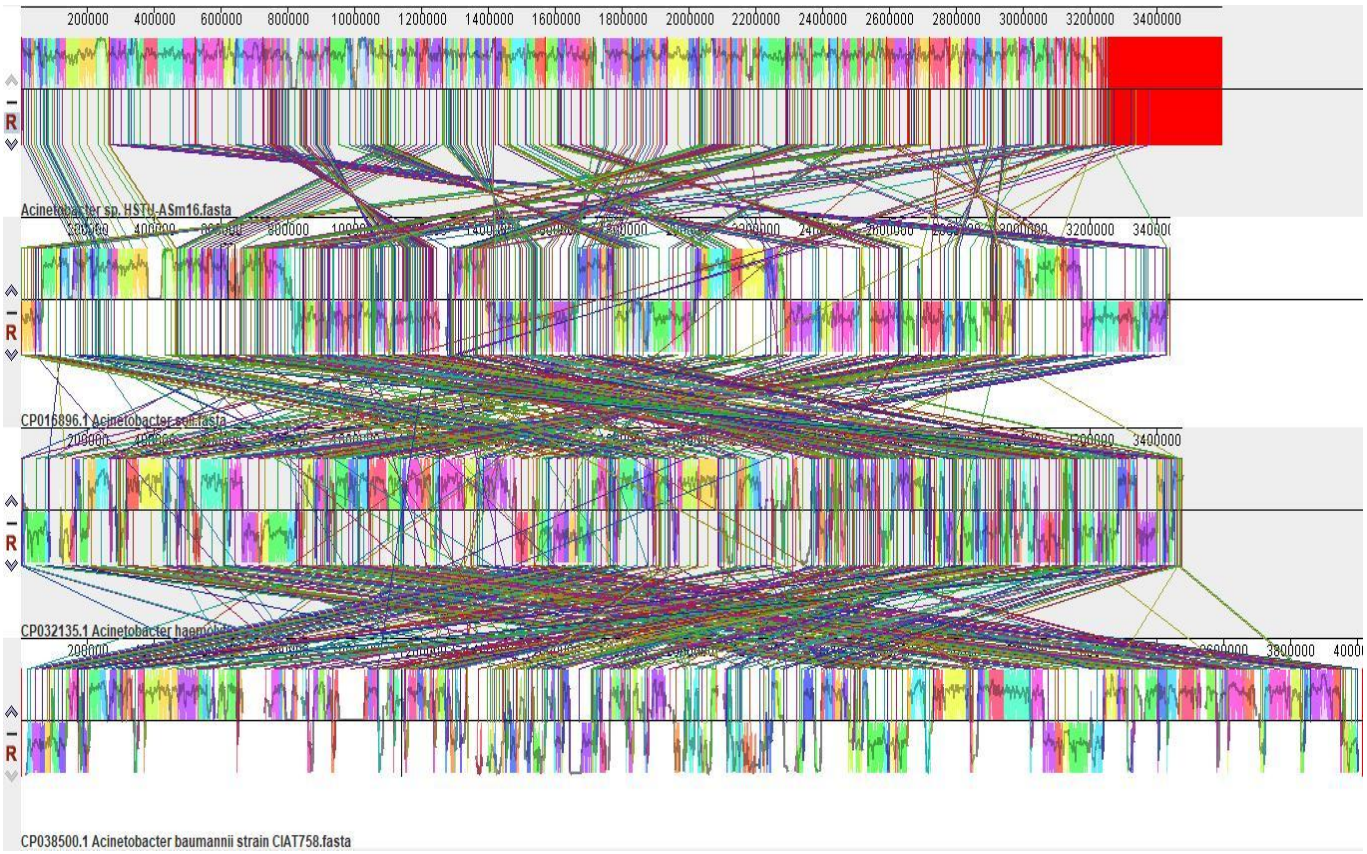

Figure 4. Progressive MAUVE of the strain *Acinetobacter* sp. HSTU-Asm16.

3.5. Plant growth-promoting (PGP) gene repertoire of *Acinetobacter* sp. HSTU-Asm16

Genome analysis of *Acinetobacter* sp. HSTU-Asm16 revealed a diverse set of genes associated with plant growth–promoting (PGP) functions, spanning nitrogen metabolism, nutrient acquisition, phytohormone biosynthesis, stress tolerance, biofilm formation, and root colonization (**Table 4**). Genes involved in nitrogen-related processes were identified, including *nifS* (cysteine desulfurase) and *nifU*, together with Fe–S cluster assembly proteins (*iscU* and *iscA*). While these genes are not sufficient for complete nitrogen fixation, they are known to support nitrogen metabolism and redox enzyme maturation. Regulatory components linked to nitrogen sensing and assimilation were also present, such as *glnK* (P-II family nitrogen regulator), *glnD* (uridylyltransferase), *gltB* (glutamate synthase large subunit), and *gltS* (sodium/glutamate symporter), indicating capacity for ammonia assimilation and nitrogen homeostasis.

Table 4. Plant growth promoting associated genes in *Acinetobacter* sp. HSTU-Asm16.

PGP activities description	Gene Name	Gene annotation	Chromosome location (HSTU-ASm16)	Locus Tag (HSTU-ASm16)	E.C. number
Nitrogen fixation	nifS	cysteine desulfurase	130466..131683	GN151_07910	2.8.1.7
	nifU	Fe-S cluster assembly protein	<1..>360	GN151_15975	-
	iscU	Fe-S cluster assembly scaffold	130009..130395	GN151_07905	-
	iscA	Fe-S cluster assembly protein	129666..129986	GN151_07900	-
Nitrosative stress	glnK	P-II family nitrogen regulator	27720..28058	GN151_10595	-
Nitrogen metabolism regulatory protein	glnD	Bifunctional uridylyl removing protein	32454..35120	GN151_11030	2.7.7.59
Ammonia assimilation	gltB	glutamate synthase large subunit	55704..60185	GN151_04120	1.4.1.13
	gltS	sodium/glutamate symporter	66337..67572	GN151_00335	
ACC deaminase	dcyD	D-cysteine desulfhydrase			4.4.1.15
	rimM	ribosome maturation factor RimM	87556..88104	GN151_04250	-
Siderophore					
Siderophore enterobactin	entC	isochorismate synthase EntC	82047..83219	GN151_06145	5.4.4.2
	rpoA	DNA-directed RNA polymerase subunit alpha	184631..185638	GN151_04780	2.7.7.6
	rpoB	DNA-directed RNA polymerase subunit beta	4013..8101	GN151_14960	2.7.7.6
Plant hormones					
IAA production	trpS	tryptophan--tRNA ligase	70493..71506	GN151_11565	6.1.1.2
	trpB	tryptophan synthase subunit beta	20270..21499	GN151_02840	4.2.1.20
	trpD	bifunctional anthranilate synthase glutamate amido transferase component	36878..37927	GN151_06640	2.4.2.18 /4.1.3.27
Phosphate metabolism	phoU	phosphate signaling complex protein PhoU	62637..63359	GN151_10755	3.5.2.6
	phoB	phosphate response regulator transcription factor PhoB	23655..24365	GN151_08150	-
	phoR	phosphate regulon sensor histidine kinase PhoR	16563..17936	GN151_12355	2.7.13.3
	ppx	Exopolyphosphatase	246977..248497	GN151_01165	3.6.1.11
	pntA	Re/Si-specific NAD(P)(+) transhydrogenase subunit alpha	287779..288906	GN151_01370	1.6.1.2
	phoQ	two-component system sensor histidine kinase PhoQ	16563..17936	GN151_12355	2.7.13.3
	efp	elongation factor P	39388..39957	GN151_13300	-
Biofilm formation	hfq	RNA chaperone Hfq	129836..130240	GN151_07050	-
Sulfur assimilation and metabolism	cysK	cysteine synthase A	41792..42790	GN151_14005	2.5.1.47
	cysM	cysteine synthase CysM	278546..279478	GN151_01325	2.5.1.47
	cysA	sulfate/thiosulfate ABC transporter ATP-binding protein CysA	182909..183970	GN151_02350	-
	cysW	sulfate/thiosulfate ABC transporter permease CysW"	183981..184871	GN151_02355	-
	cysN	sulfate adenylyl transferase subunit CysN	57116..58729	GN151_09470	2.7.7.4
	cysD	sulfate adenylyl transferase subunit CysD	58774..59682	58774..59682	2.7.7.4
	cysH	Phosphor adenosine phosphosulfate reductase	43413..44147	GN151_00220	1.8.4.8
	cysE	serine O-acetyltransferase	48809..49618	GN151_11085	2.3.1.30
	cysK	cysteine synthase A	278546..279478	GN151_01325	2.5.1.47
	cysS	cysteine--tRNA ligase	82305..83726	GN151_10470	6.1.1.16
Synthesis of resistance inducers					
Methanethiol	metH	methionine synthase	85678..89364	GN151_09585	2.1.1.13
2,3-butanediol	ilvB	acetolactate synthase large subunit			-
	ilvN	acetolactate synthase small subunit	305246..305737	GN151_01435	2.2.1.6
	ilvA	Serine, threonine dehydratase	87259..88797	GN151_07690	4.3.1.19
	ilvC	ketol-acid reductoisomerase	304197..305213	GN151_01430	1.1.1.86
	ilvY	HTH-type transcriptional activator IlvY			-
	ilvD	Dihydroxy-acid dehydratase	9229..10914	GN151_12605	4.2.1.9
	ilvM	acetolactate synthase 2 small subunits	305246..305737	GN151_01435	2.2.1.6
Isoprene	ispE	4-(cytidine5'-diphospho)-2-C-methyl-D-erythritol kinase	38731..39552	GN151_11420	2.7.1.148

	gcpE/ ispG	flavodoxin-dependent (E)-4-hydroxy-3-methylbut-2-enyl-diphosphate synthase	95683..96798	GN151_03190	1.17.7.1
Symbiosis-related	pyrC	Dihydroorotase	742..1776	GN151_08675	3.5.2.3
	tatA	Sec-independent protein translocase subunit TatA	137790..138011	GN151_03360	-
	bacA	undecaprenyl-diphosphate phosphatase	20717..21517	GN151_10175	3.6.1.27
Oxidoreductase	osmC	peroxiredoxin OsmC	12737..13300	GN151_14510	1.11.1.15
	gpx	glutathione peroxidase			1.11.1.9
Hydrolase	ribA	GTP cyclohydrolase II	61944..62546	GN151_08340	3.5.4.25
	folE	GTP cyclohydrolase I FolE	29508..30101	GN151_06610	3.5.4.16
	bglX	beta-glucosidase BglX			3.2.1.21
Root colonization Chemotaxis	cheB	chemotaxis-specificprotein-glutamate methyltransferase CheB			3.1.1.61
Adhesin production	pgaB	poly-beta-1,6-N-acetyl-D-glucosamine N-deacetylase PgaB	101099..103174	GN151_09650	3.5.1.-
	pgaD	poly-beta-1,6-N-acetyl-D-glucosamine biosynthesis protein	99382..99795	GN151_09640	-

Multiple genes associated with phosphate metabolism and regulation were detected, including the phosphate signaling and uptake regulators *phoU*, *phoB*, *phoR*, and *phoQ*, along with *ppx* encoding exopolyphosphatase. The presence of *pntA*, encoding NAD(P)+ transhydrogenase, further suggests a role in maintaining redox balance during nutrient-limited conditions. The genome also encoded components related to iron acquisition, including the enterobactin biosynthesis gene *entC*, supporting potential siderophore-mediated iron scavenging. Genes involved in plant hormone–related pathways, particularly indole-3-acetic acid (IAA) precursor metabolism, were identified through the presence of tryptophan biosynthesis and utilization genes (*trpS*, *trpB*, and *trpD*), which are commonly associated with bacterial IAA production routes.

Genes implicated in ACC deaminase activity and stress modulation, such as *dcyD* (D-cysteine desulfhydrase), were present, potentially contributing to ethylene regulation under plant stress conditions. Additionally, oxidative and nitrosative stress response genes, including *osmC* (peroxiredoxin) and *gpx* (glutathione peroxidase), suggest an enhanced capacity to tolerate reactive oxygen species within the plant environment. A comprehensive set of genes involved in sulfur assimilation and metabolism was identified, including *cysA*, *cysW*, *cysN*, *cysD*, *cysH*, *cysE*, *cysK*, *cysM*, and *cysS*, supporting cysteine and methionine biosynthesis and sulfur uptake. Genes associated with the synthesis of volatile and resistance-inducing compounds, such as *metH* (methionine synthase) and enzymes of the 2,3-butanediol biosynthetic pathway (*ilvB, ilvN, ilvA, ilvC, ilvD,* and *ilvM*), were also detected. Pathways linked to isoprene biosynthesis were represented by *ispE* and *ispG (gcpE)*, while genes associated with symbiosis and host interaction, including *pyrC*, *tatA*, and *bacA*, were present. The strain also encoded several hydrolases and oxidoreductases, such as *ribA*, *folE*, and *bglX*, which may contribute to metabolic versatility in the rhizosphere. Finally, genes involved in biofilm formation and root colonization were identified, including *efp* and *hfq*, as well as chemotaxis (*cheB*) and adhesion-related genes (*pgaB* and *pgaD*), supporting the potential for effective root surface attachment and endophytic colonization.

3.6. Abiotic Stress–Related Genes Identified in the Genome of *Acinetobacter* sp. HSTU-ASm16

Genome annotation of *Acinetobacter* sp. HSTU-ASm16 identified multiple genes associated with responses to abiotic stresses (**Table 5**). Genes encoding heat shock and protein quality control systems were detected, including *groL* (chaperonin GroEL), *dnaK* and *dnaJ* (molecular chaperones), *grpE* (nucleotide exchange factor), and the heat shock sigma factor *rpoH*. Additional stress-associated genes included *smpB*, encoding the SsrA-binding protein, and *lepA*, encoding elongation factor 4. Genes associated with heavy metal resistance were present. The arsenic resistance–related genes *arsB* (arsenical efflux pump) and *arsH* (arsenical resistance protein) were identified, along with *chrA*, encoding a chromate efflux transporter. Genes involved in metal ion homeostasis included *htpX*, encoding a membrane-associated protease, and *cobA*, encoding uroporphyrinogen-III C-methyltransferase. Multiple genes related to osmotic and drought stress were identified. These included *proA* (glutamate-5-semialdehyde dehydrogenase), *proB* (glutamate 5-kinase), *proP* (glycine betaine/L-proline transporter), and *proS* (proline–tRNA ligase). Genes involved in compatible solute biosynthesis were also present, including *betA* (choline dehydrogenase) and *betB* (betaine-aldehyde dehydrogenase). In addition, the two-component system sensor histidine kinase *kdbD* was detected.

Table 5. Genes involved in different abiotic stresses available in *Acinetobacter* sp. HSTU- ASm16 genome.

Activity description	Gene Name	Gene annotation	Chromosome location (HSTU-ASm16)	Locus Tag (HSTU-ASm16)	E.C. number
Heat Shock protein	*smpB*	SsrA-binding protein SmpB	48842..49318	GN151_11465	-
	groL	chaperonin GroEL	24592..26226	GN151_01625	-
	dnaJ	molecular chaperone DnaJ	25746..26864	GN151_12660	-
	dnaK	molecular chaperone DnaK	5934..7880	GN151_13390	-
	rpoH	RNA polymerase sigma factor RpoH	46074..46943	GN151_07455	-
	lepA	elongation factor 4	195684..197501	GN151_02410	3.6.5.n1
	grpE	nucleotide exchange factor GrpE	5260..5814	GN151_13385	-
Heavy metal resistance					
Arsenic tolerance	*arsB*	arsenical efflux pump membrane protein ArsB	5908..6951	GN151_14260	-
	arsB	arsenical efflux pump membrane protein ArsB	5908..6951	GN151_14260	-
	arsH	Arsenical reseistance protein arsH	6957..7661	GN151_14265	-
Chromium resistance	*chrA*	Chromate efflux transporter	3826..5013	GN151_10895	-
Magnesium transport	*cobA*	uroporphyrinogen-III C-methyltransferase	20406..21800	20406..21800	-
Zinc homeostasis	*htpX*	protease HtpX	32333..33238	GN151_01650	3.4.24.-
Drought resistance	*proA*	glutamate-5-semialdehyde dehydrogenase	108655..109920	GN151_03250	1.2.1.41
	proB	glutamate 5-kinase	217255..218388	GN151_02525	2.7.2.11
	proP	glycine betaine/L-proline transporter ProP	43930..45411	GN151_11830	-
	proS	proline--tRNA ligase	94025..95737	GN151_00475	6.1.1.15
	betA	choline dehydrogenase	157679..159337	GN151_06435	1.1.99.1
	betB	betaine-aldehyde dehydrogenase	159427..160899	GN151_06440	1.2.1.8
	kdbD	two-component system sensor histidine kinase KdbD	16563..17936	GN151_12355	2.7.13.3

3.7. Genes associated with pesticide degradation

Genome annotation of *Acinetobacter* sp. HSTU-ASm16 revealed multiple genes encoding enzymes putatively involved in pesticide degradation and xenobiotic metabolism (**Table 6**). These genes were distributed throughout the chromosome, indicating that the pesticide-degrading potential is genomically integrated rather than confined to a specific operon or genomic island. The genome harbored the ampD gene encoding 1,6-anhydro-N-acetylmuramyl-L-alanine amidase (EC 3.5.1.28), a member of the amidohydrolase superfamily known for catalyzing amide bond cleavage in diverse xenobiotic compounds. In addition, several amidohydrolase family proteins (GN151_06015, GN151_07410, and GN151_11120) were identified, suggesting a broad enzymatic capacity for hydrolyzing organophosphate- and carbamate-like pesticides.

Genes involved in aromatic compound metabolism were also detected, including paaC, encoding phenylacetate-CoA oxygenase subunit PaaC, which may facilitate the transformation of aromatic intermediates generated during pesticide degradation. The presence of pepA (leucyl aminopeptidase; EC 3.4.11.1) further suggests a role in downstream processing of degradation products.

Table 6. Genes associated with pesticide degradation available in *Acinetobacter* sp. HSTU-ASm16 genome.

Activity description	Gene Name	Gene annotation	Chromosome location (HSTU-ASm16)	Locus Tag (HSTU-ASm16)	E.C. number
Pesticide degrading	*ampD*	1,6-anhydro-N-acetylmuramyl-L-alanineamidase	11648..12238	GN151_14070	3.5.1.28
-	*glpB*	glycerol-3-phosphate dehydrogenase subunit	18507..20024	GN151_01600	1.1.5.3
	pepA	leucyl aminopeptidase	34288..35736	GN151_10635	3.4.11.1
	paaC	phenylacetate-CoA oxygenase subunit PaaC	92071..92826	GN151_09055	
	-	Amidohydrolase	47408..48562	GN151_06015	
	-	amidohydrolase family protein	38596..39831	GN151_07410	
	-	amidohydrolase family protein	57071..58504	GN151_11120	
	-	Glycerophosphodiester phosphodiesterase	254..1393	GN151_10480	
	-	glycerophosphodiester phosphodiesterase	25094..25810	GN151_02860	
	-	3',5'-cyclic-nucleotide phosphodiesterase	23281..24072	GN151_01615	

Moreover, the genome encoded glpB (glycerol-3-phosphate dehydrogenase subunit; EC 1.1.5.3), along with multiple glycerophosphodiester phosphodiesterases and a 3′,5′-cyclic-nucleotide phosphodiesterase. These enzymes are associated with phosphoester bond cleavage and are particularly relevant to the biodegradation of organophosphate pesticides. Given that diazinon contains phosphoester linkages, these phosphodiesterase-like enzymes may contribute to its initial hydrolytic transformation, either directly or through functional promiscuity reported for related hydrolases. Thus, the presence of diverse hydrolases, oxygenases, and phosphodiesterases highlights the strong genetic potential of *Acinetobacter* sp. HSTU-ASm16 to participate in multi-step biodegradation pathways of structurally diverse pesticides.

3.8. Virtual screening (docking) analysis of the model proteins with pesticides

Figure 5 illustrates the virtual screening of pesticide-degrading model proteins from *Acinetobacter* sp. HSTU-Asm16, based on their predicted binding affinities (kcal/mol). Virtual screening, employing molecular docking simulations, estimates the interaction strength between ligands and target proteins, with more negative binding affinity values indicating stronger interactions. Seven model proteins were analyzed: AmpD, PepA, two Amidohydrolase family proteins (38596–39831 and 57071–58504), GlpB, PaaC, and Glycerophosphodiester phosphodiesterase (25094–25810). Among these, the Amidohydrolase family protein (57071–58504) exhibited the strongest median binding affinity (-6.4 kcal/mol), suggesting the formation of the most stable protein–pesticide complexes. The other Amidohydrolase protein (38596–39831) had a median binding affinity of -5.2 kcal/mol. GlpB and PaaC demonstrated moderate binding affinities of -6.0 kcal/mol and -5.6 kcal/mol, respectively, consistent with their known roles in aromatic compound and glycerophosphodiester degradation. AmpD and PepA displayed median affinities of -5.0 kcal/mol and -4.8 kcal/mol, respectively, with PepA showing a notable outlier at -7.4 kcal/mol, indicating potential strong interactions with specific pesticides. Similarly, Glycerophosphodiester phosphodiesterase exhibited an outlier at -7.2 kcal/mol. Overall, these results identify the Amidohydrolase family protein (57071–58504) as the most promising candidate for pesticide degradation in *Acinetobacter* sp. HSTU-Asm16. The observed strong outliers for PepA and Glycerophosphodiester phosphodiesterase highlight additional proteins that may contribute to efficient pesticide breakdown, warranting further experimental validation.

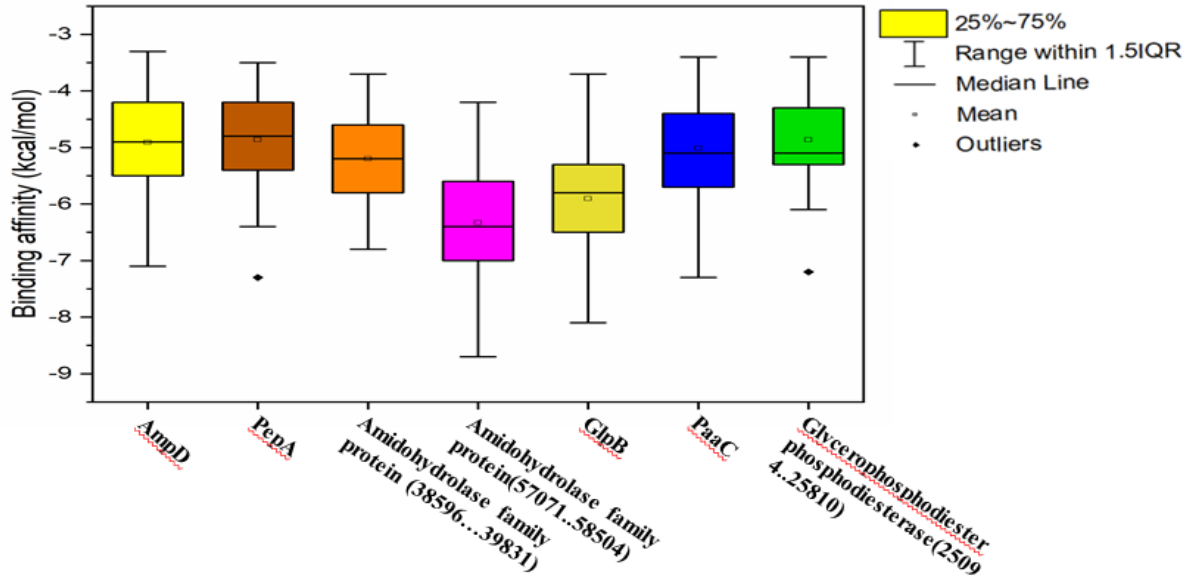

Figure 5. virtual screening of pesticides degrading model protein-pesticides complex of the strain *Acinetobacter* sp. HSTU-Asm16.

3.9. Molecular docking and visualization of the pesticides-model putative pesticides degrading proteins

The conventional hydrogen bond interaction was observed for Ser41 and ASN39 with the side chain of the benzene ring attached, the O-atom, and the N-H atom of the phosphodiester of pyraclofos compound, while PRO169, PHE68, and LEU64 formed alkyl and π-alkyl bonds with the Cl-atom of pyraclofos, and Tyr51 formed. The AmpD protein and Phoxim

insecticide docked complex ligand interactions were observed by the different residues (**Figure 6A**). In particular, Phe317 with Glu315 provided an attractive charge interaction with the phosphate atom. In addition, conventional hydrogen bond and pi sigma interactions were observed with the His45 and Ser46 residues. The interaction distances among the residues of the catalytic site were recorded within <3.9 Å. Another set of interactions is responsible for GlpB's high affinity for Diazinon (**Figure 6B**). Moreover, alpha/beta fold hydrolase (NR044454) protein-diazinon docked complex demonstrated the interaction with multiple residues (**Figure 6C**). In particular, conventional H-bond were made by His224, Ser231 to the O-atom of diazinon compound. Besides, Val346 with Lys431 also formed a conventional hydrogen bond. Multiple residues were interacted by alkyl, pi-alkyl, and carbon-hydrogen bonds namely, Met123, Leu208, Ile137, Phe133, His231 and Leu31 sequentially.

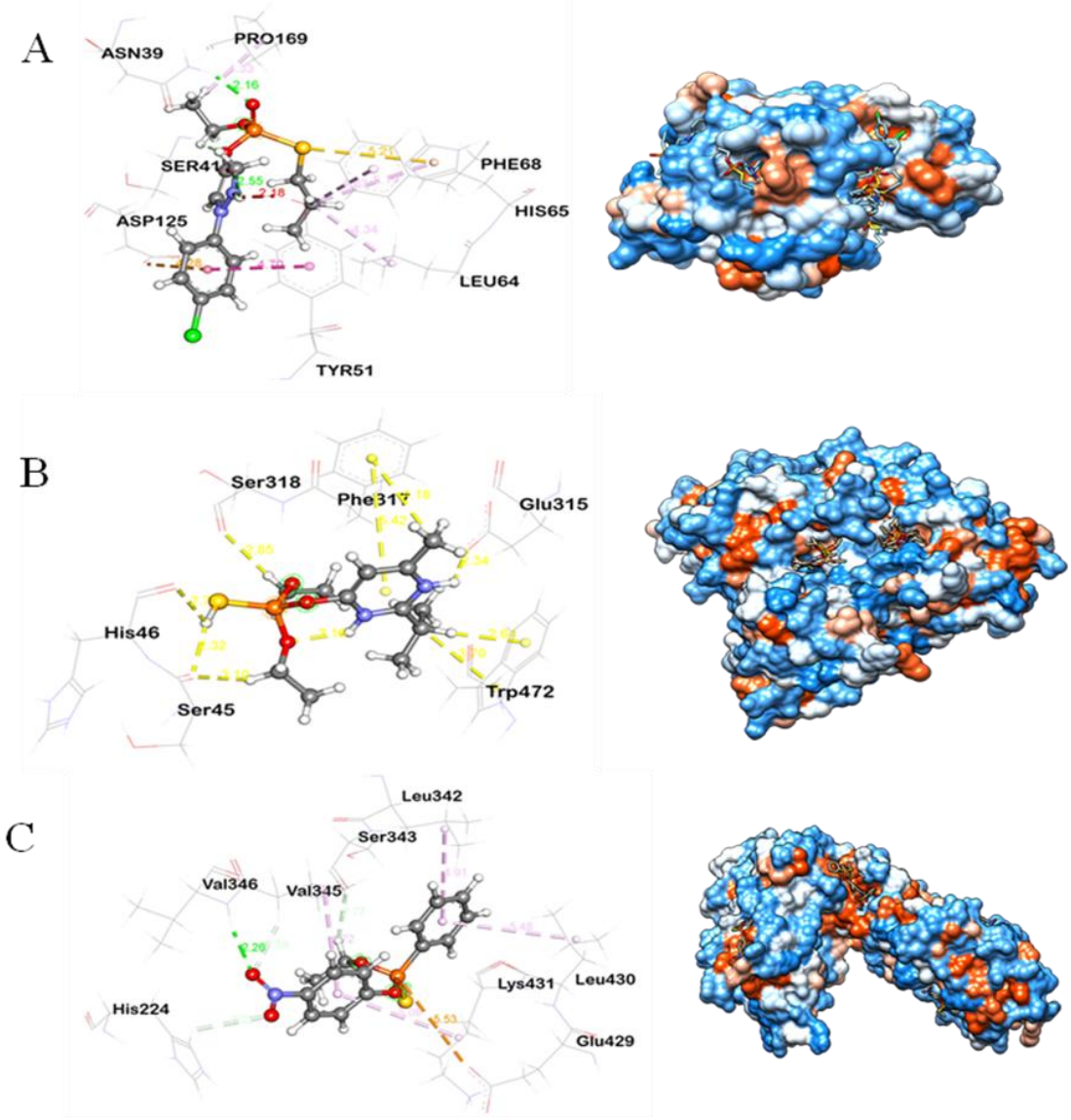

Figure 6. **(A)** Molecular docking visualization of the AmpD protein with Phoxim insecticide. **(B)** Molecular docking visualization of the GlpB with diazinon insecticide. **(C)** Molecular docking visualization of the PepA with EPN insecticide.

4. DISCUSSION

The integrated biochemical and genomic characterization of *Acinetobacter* sp. HSTU-Asm16 highlights its potential as a multifunctional rice endophyte with both plant growth-promoting (PGP) traits and the genomic capacity to participate in organophosphate pesticide degradation. Biochemically, HSTU-Asm16 showed catalase and oxidase activity, citrate utilization, carbohydrate fermentation, and production of extracellular hydrolases (amylase, protease, xylanase), traits commonly associated with metabolically flexible endophytes that can access diverse carbon sources and modify plant cell wall components to facilitate colonization and nutrient exchange. The absence of detectable CMCase activity, while other hydrolases are retained, suggests a significant microbial specialization towards particular polysaccharide substrates rather than broad cellulolysis [41]. This targeted degradation indicates that the microbe has evolved to efficiently process specific complex carbohydrates, a trait observed in organisms thriving in competitive environments [42]. Such enzymatic specialization fosters commensal or mutualistic interactions with host plants by allowing the microbe to access nutrients without aggressive tissue maceration. This strategic metabolic approach benefits both the microbe and the plant by enabling nutrient acquisition or cell wall modification for colonization, promoting a balanced and symbiotic relationship [43].

Whole-genome phylogenetic reconstruction, leveraging both read-mapping and reference alignment approaches, robustly positioned HSTU-Asm16 in close evolutionary proximity to *Acinetobacter soli* strains. This phylogenetic placement was further corroborated by analyses of housekeeping gene trees [34]. To ascertain the genetic relatedness with greater resolution, the JSpeciesWS platform was employed to generate Average Nucleotide Identity and other pairwise genomic metrics. ANI, a robust method for bacterial species demarcation, typically shows ≥95% identity among strains of the same species [44, 45]. Concurrently, digital DNA-DNA hybridization (dDDH) values and their associated confidence intervals were obtained using the Genome-to-Genome Distance Calculator, a tool commonly used for prokaryotic species delineation [46]. Collectively, the results from these platforms affirmed HSTU-Asm16's strong affinity to *A. soli*, while also revealing significant strain-level differentiation across multiple comparisons. Further enhancing the phylogenetic resolution, REALPHY-derived whole-genome phylogenies, inferred from mapped reference alignments, provided intricate details of genome-scale evolutionary relationships, contributing to a comprehensive understanding of HSTU-Asm16's taxonomic position [47].

The extensive genome rearrangements, horizontal gene transfer, and the acquisition of mobile genetic elements observed in *HSTU-Asm16* are hallmarks of adaptive strategies in environmental *Acinetobacter* species. This genomic plasticity enables bacteria to thrive in diverse and dynamic environments and to form host associations [48-49]. Comparative genomic studies on *Acinetobacter baumannii* have shown that pangenome analysis can reveal structural variations and constant genetic permutation among strains, indicating high genomic plasticity [50-51]. Similarly, research on *Acinetobacter haemolyticus* has identified chromosomes organized into syntenic blocks interspersed with hypervariable regions rich in unique gene families and signals of horizontal gene transfer [52]. These findings support the idea that pangenome and synteny analyses are crucial for understanding the evolutionary dynamics of bacterial genomes. Although the isolate does not represent a new species, its distinct genomic repertoire related to pesticide biodegradation highlights its strain-level novelty and functional relevance.

Bacterial genome diversification and the development of niche-specific functions are often driven by continuous processes of niche exploration, diversification, and adaptation [53]. Comparative genomics helps reveal these adaptive mechanisms, particularly in host-niche specialization [54]. The ability of *Acinetobacter* species to adapt to a wide range of environmental conditions is linked to their genomic plasticity [55] with niche-specific adaptive mutations and genes mediating fitness in different habitats [48]. Bacterial genome rearrangements, including gene loss, duplication, and acquisition, are significantly influenced by horizontal gene transfer, frequently mediated by mobile genetic elements like plasmids and transposons [55]. The *Acinetobacter* genus, being ancient and diverse, undergoes outstanding diversification largely through horizontal transfer and allelic recombination at specific hotspots [56]. This process, including conjugation, is a major contributor to bacterial genome plasticity, evolution, and adaptation, particularly in the transfer of traits like multi-drug resistance [57]. *Acinetobacter baumannii*, for instance, is noted for its high genomic plasticity and its predisposition to exchange MGEs through HGT [58].

The results highlights that gene mining of HSTU-Asm16 revealed several key plant growth-promoting activities, including nitrogen fixation, siderophore biosynthesis for iron acquisition, indole-3-acetic acid synthesis, and ACC deaminase for hormone modulation, along with capabilities for phosphate solubilization and sulfur assimilation. These features, supported by genes for chemotaxis, adhesion, and biofilm formation, enable efficient root colonization and stable endophytism, consistent with findings on other endophytic bacteria [41,59 ,60]. Additionally, HSTU-Asm16 possesses a notable complement of organophosphate-degrading enzymes, such as carboxylesterases, amidohydrolases, phosphodiesterases, and organophosphorus hydrolase homologs, indicating its potential in bioremediation of organophosphate contaminants through enzymatic breakdown [61-63]. Functionally, gene mining revealed multiple loci associated with classical plant growth-promoting activities: (i) nitrogen-related genes (nif clusters and electron transport components for alternative nitrogenases), (ii) siderophore biosynthesis pathways such as enterobactin-type systems for iron acquisition, (iii) indole-3-acetic acid synthetic pathways and ACC deaminase for modulation of plant hormone signaling, and (iv) phosphate solubilization and sulfur assimilation genes that can improve nutrient availability. The presence of chemotaxis, adhesion, and biofilm formation genes supports efficient root colonization and stable endophytism. These features align with reports that endophytic bacteria often carry suites of genes enabling nutrient exchange, stress amelioration, and intimate host colonization [41, 64]. Of special interest is HSTU-Asm16's complement of putative organophosphate-degrading enzymes. Genome mining detected genes encoding carboxylesterases, amidohydrolases, phosphodiesterases, and homologs of organophosphorus hydrolase. These microbial enzymes are recognized for their role in the bioremediation of organophosphate compounds, which are often environmental contaminants [61, 62]. Molecular docking provided mechanistic plausibility for predicted biodegradation. Docking of representative organophosphate ligands, such as paraoxon [65] and chlorpyrifosmethyl oxon [66] against candidate hydrolases yielded energetically favorable poses with canonical catalytic residues (Ser/His/Asp triads and metal-binding motifs) forming hydrogen bonds, electrostatic contacts, and hydrophobic stabilization within distances consistent with catalysis (<4 Å). These observed interactions mirror catalytic geometries described in biochemical studies of phosphotriesterases and related hydrolases [67]. While *in-silico* docking cannot replace biochemical assays, the concordance between genomic presence of candidate hydrolase genes and favorable docking interactions, as explored through computational enzymology [68], strengthens the inference that HSTU-Asm16

encodes functional degradative pathways. Docking scores were interpreted as relative indicators of binding propensity rather than absolute binding free energies. A cutoff value of ≤ –7.0 kcal/mol was applied to prioritize biologically relevant enzyme–ligand complexes, as this threshold is commonly used in virtual screening and approximately corresponds to micromolar-range binding affinity. This criterion is appropriate for environmental substrates such as pesticides, which are not optimized for high-affinity binding. All selected complexes were further evaluated based on binding pose stability and interactions with conserved catalytic residues. Although this study did not experimentally verify diazinon degradation by the investigated strain, several endophytic bacteria and phylogenetically related taxa have previously been reported to metabolize diazinon under minimal nutrient conditions. In this context, the present genome-centric and molecular docking analyses provide predictive and mechanistic insight into the potential of the strain to interact with diazinon at the enzyme level. The identification of conserved organophosphate-degrading enzyme families, coupled with favorable ligand–protein interactions observed in silico, suggests a genetically encoded capacity for diazinon transformation. Nevertheless, strain-specific biochemical validation using GC–MS/MS and metabolite profiling is required and will be addressed in future experimental investigations.

Taken together, HSTU-Asm16 represents a genomically equipped endophyte with a dual capacity. It carries genes for nutrient acquisition and stress resistance that likely support plant growth under diverse conditions, and it harbors enzyme candidates with plausible mechanisms for organophosphate turnover [69]. These dual capacities argue for its potential deployment as a bioinoculant that could both boost rice productivity and contribute to *in-situ* pesticide detoxification an attractive strategy in integrated pest and soil health management [70]. However, to translate genomic and *in-silico* predictions into application, targeted biochemical validation is required: heterologous expression and kinetic characterization of the candidate hydrolases, gene knockouts or transcriptomics under pesticide exposure, and greenhouse/field trials to measure colonization, plant responses, and pesticide dissipation kinetics [71].

5. CONCLUSION

Acinetobacter sp. HSTU-Asm16 is a metabolically versatile, genomically distinct endophytic strain from rice that combines plant growth-promoting features with a predicted enzymatic toolkit for organophosphate degradation. Comparative genomics (ANI/dDDH, pangenome and synteny analyses) places the strain within the *A. soli*-related clade but highlights accessory genomic regions and rearrangements indicative of strain-level novelty. Genome annotation uncovered genes linked to nutrient acquisition, stress tolerance, colonization and multiple classes of hydrolases implicated in OP pesticide degradation; molecular docking supports plausible active-site interactions with representative OP compounds. Future work should prioritize biochemical validation of the hydrolases, gene expression studies under pesticide challenge, and controlled plant assays to confirm PGP efficacy and bioremediation potential before field application. Altogether, HSTU-Asm16 is a promising candidate for integrated strategies aimed at improving rice health while mitigating chemical pesticide residues. We emphasize that docking results provide preliminary, comparative insights into enzyme–substrate compatibility and do not substitute for molecular dynamics simulations or experimental validation, which will be addressed in further studies for sustainable green agrosystem.

ACKNOWLEDGEMENTS

The authors gratefully acknowledge IRT of Hajee Mohammad Danesh Science and Technology University (HSTU), for financial support. We also thank all contributors for their valuable roles in the preparation of this manuscript. In addition, this study addresses about 10% AI-assisted text for arranging and formatting the manuscript following the journal policy.

FUNDING SOURCES

This research was supported by the grants from the Institute of Research and Training (IRT)-Hajee Mohammad Danesh Science and Technology University (HSTU) in fiscal year 2021-2022 at Dinajpur, Bangladesh.

CONFLICTS OF INTEREST

The authors declare no conflicts of interest.

ETHICS STATEMENT

This study did not involve any experiments on human participants or animals; therefore, formal written informed consent was not required by the Institutional Review Board. All figures in this study were created; therefore, no permission for reuse is required for any figure presented herein.

DATA AVAILABILITY STATEMENT

The assembled and annotated genome sequence was deposited in the NCBI and provided accession number as *Acinetobacter soli* strain HSTU-ASm16 (Accession number: JARWII000000000, BioSample: SAMN34186007; BioProject: PRJNA955703).

REFERENCES

1. Barman DN, Haque MA, Islam SMA, Yun HD, Kim MK. Cloning and expression of ophB gene encoding organophosphorus hydrolase from endophytic *Pseudomonas sp.* BF1-3 degrades organophosphorus pesticide chlorpyrifos. *Ecotoxicol Environ Saf*. 2014; 108:135-41. doi: 10.1016/j.ecoenv.2014.06.023
2. Malhotra H, Kaur S, Phale PS. Conserved metabolic and evolutionary themes in microbial degradation of carbamate pesticides.*Front Microbiol*. 2021; *12*. https://doi.org/10.3389/fmicb.2021.648868
3. Roy MK, Roy S, Binduraz B, Afrin L, Haque MA. Pesticide-associated health and environmental risks and the role of biofertilizers in sustainable agriculture. J Biosci Public Health. 2025;1(3):16–27. doi:10.5455/JBPH.2025.12
4. Sharma A, Kumar V, Handa N, Bali S, Kaur R, Khanna K, Thukral AK, Bhardwaj R. Potential of endophytic bacteria in heavy metal and pesticide detoxification. In: Egamberdieva, D., Ahmad, P. (eds) Plant Microbiome: Stress Response. Microorganisms for Sustainability, vol 5. Springer, Singapore. https://doi.org/10.1007/978-981-10-5514-0_14
5. Das SR, Haque MA, Akbor MA, Mamun AA, Debnath GC, Hossain MS, Hasan Z, Rahman A, Islam MA, Hossain MAA, Yesmin S, Nahar M NEN,Cho KM. Organophosphorus insecticides mineralizing endophytic and rhizospheric soil bacterial consortium influence eggplant growth-promotion. *Arch. Microbiol*. 2022;*204*(3). doi.org/10.1007/s00203-022-02809-w
6. Mithu MMU, Shormela SA, Islam MS, Mubarak M. FTIR analysis of pesticide active ingredients in seasonal vegetables: ensuring food safety and raising awareness. J Glob Innov Agric Sci. 2025; 13:139–147. doi:10.22194/JGIAS/25.1463
7. Prodhan MY, Rahman MB, Rahman A, Akbor MA, Ghosh S, Nahar MNEN, Simo, Shamsuzzoha M, Cho KM, Haque MA. Characterization of Growth-Promoting Activities of Consortia of Chlorpyrifos Mineralizing Endophytic Bacteria Naturally

Harboring in Rice Plants-A Potential Bio-Stimulant to Develop a Safe and Sustainable Agriculture. *Microorg*. 2023;*11*(7): 1821. https://doi.org/10.3390/microorganisms11071821

8. Lopes AR, Bunin ES, Viana AT, Froufe,HJC, Muñoz-Mérida A, Pinho D, Figueiredo J, Barroso C, Vaz-Moreira I, Bellanger X, Egas C, Nunes OC. In silico prediction of the enzymes involved in the degradation of the herbicide molinate by *Gulosibacter molinativorax* ON4T. *Sci Rep*. 2022; *12*(1). https://doi.org/10.1038/s41598-022-18732-5

9. Kour D, Kaur T, Devi R, Chaubey KK, Yadav AN. Co-inoculation of nitrogen fixing and potassium solubilizing *Acinetobacter sp.* for growth promotion of onion (*Allium cepa*). *Biologia*. 2023;*78*(9):2635. https://doi.org/10.1007/s11756-023-01412-8

10. Reyes-Castillo A, Gerding M, Oyarzúa P, Zagal E, Gerding J, Fischer S. Plant growth-promoting rhizobacteria able to improve NPK availability: selection, identification and effects on tomato growth. *Chil. J. Agric. Res*. 2019;*79*(3):473. https://doi.org/10.4067/s0718-58392019000300473

11. Rey-Velasco X, Lucena T, Belda A, Gasol JM, Sánchez O, Arahal DR, Pujalte MJ. Genomic and phenotypic characterization of 26 novel marine bacterial strains with relevant biogeochemical roles and widespread presence across the global ocean. *Front Microbiol*. 2024;*15*. https://doi.org/10.3389/fmicb.2024.1407904

12. Mithu MMU, Shormela SA, Abdullah ATM, et al. Exploring heavy metal bioaccumulation in vegetables: unraveling environmental pollutants' impact on agricultural produce and human health. Biol Trace Elem Res. 2025. doi:10.1007/s12011-025-04871-z

13. Zhao T, Chen P, Zhang L, Zhang L, Gao Y, Ai S, Liu H, Liu X. Heterotrophic nitrification and aerobic denitrification by a novel *Acinetobacter sp*. TAC-1 at low temperature and high ammonia nitrogen. *Bioresour. technol*. 2021; *339*:125620. https://doi.org/10.1016/j.biortech.2021.125620

14. Zhong Y, Xia H. Characterization of the nitrogen removal potential of two newly isolated *Acinetobacter* strains under low temperature. Water. *2023; 15*(16): 2990. https://doi.org/10.3390/w15162990

15. Mao J, Zhao R, Li Y, Qin W, Wu S, Xu W, Jin P, Zheng Z. Nitrogen removal capability and mechanism of a novel low-temperature-tolerant simultaneous nitrification-denitrification bacterium *Acinetobacter kyonggiensis* AKD4. *Front Microbiol*. 2024:*15*1349152. https://doi.org/10.3389/fmicb.2024.1349152

16. Rokhbakhsh-Zamin F, Sachdev D, Pour NK, Engineer AS, Pardesi KR, Zinjarde S, Dhakephalkar PK, Chopade BA. Characterization of *plant-growth-promoting traits of Acinetobacter Species Isolated from Rhizosphere of Pennisetum glaucum*. *J Microbiol Biotechnol.* 2011;*21*(6): 556. https://doi.org/10.4014/jmb.1012.12006

17. He D, Wan W. Phosphate-solubilizing bacterium *acinetobacter pittii* gp-1 affects rhizosphere bacterial community to alleviate soil phosphorus limitation for growth of soybean (*glycine max*). *Front Microbiol*. 2021; *12*:737116. https://doi.org/10.3389/fmicb.2021.737116

18. Patel P, Shah R, Modi K. Isolation and characterization of plant growth promoting potential of *Acinetobacter* sp. RSC7 isolated from *Saccharum officinarum* cultivar Co 671. *Exp. Biol. Agric. Sci.*2017***;****5*(4), 483. https://doi.org/10.18006/2017.5(4).483.491

19. Xie J, Yan Z, Wang G, Xue W, Li C, Chen X, Chen D. A bacterium isolated from soil in a karst rocky desertification region has efficient phosphate-solubilizing and plant growth-promoting ability. *Front Microbiol*. 2021; *11*. https://doi.org/10.3389/fmicb.2020.625450

20. Islam T, Deora A, Hashidoko Y, Rahman A, Ito T, Tahara S. isolation and identification of potential phosphate solubilizing bacteria from the rhizoplane of *Oryza sativa* L. cv. BR29 of Bangladesh. *Naturforsch*.2007; *62*: 103. https://doi.org/10.1515/znc-2007-1-218

21. Betoudji F, Rahman TAE, Miller MJ, Ghosh M, Jacques M, Bouarab K, Malouin,F. A siderophore analog of *fimsbactin* from *acinetobacter* hinders growth of the phytopathogen *pseudomonas syringae* and induces systemic priming of immunity in arabidopsis thaliana. *Pathogens*. 2020; *9*(10): 806. https://doi.org/10.3390/pathogens9100806

22. Knauf A, Powers MJ, Herrera CM, Trent MS, Davies BW. Acinetobactin-mediated inhibition of commensal bacteria by *Acinetobacter baumannii*. *mSphere*. 2022;*7*(1). https://doi.org/10.1128/msphere.00016-22

23. Jangra A, Kumar K, Maikhuri S, Bhandari MS, Pandey S, Singh H, Barthwal S. Unveiling stress-adapted endophytic bacteria: Characterizing plant growth-promoting traits and assessing cross-inoculation effects on *Populus deltoides* under abiotic stress. *Plant Physiol Biochem*. 2024;*210*: 108610. https://doi.org/10.1016/j.plaphy.2024.108610

24. Sharker B, Islam MA, Hossain MAA, Ahmad I, Al Mamun A, Ghosh S, Haque MA. (2023). Characterization of lignin and hemicellulose degrading bacteria isolated from cow rumen and forest soil: Unveiling a novel enzymatic model for rice straw deconstruction. *Sci Total Environ*. 2023;904: 166704. https://doi.org/10.1016/j.scitotenv.2023.166704

25. Gupta S, Mandal A, Ghosh A, Kundu A, Saha S, Singh A, Dutta A. Evaluating the insecticidal potential of alkaloids for the management of *Thrips palmi*: in vivo and in silico perspectives. *Sci Rep*.2024; *14*(1). https://doi.org/10.1038/s41598-024-77236-6

26. Liu J, Liu M, Yao Y, Wang J, Li Y, Li G, Wang Y. Identification of novel potential β-n-acetyl-d-hexosaminidase inhibitors by virtual screening, molecular dynamics simulation and MM-PBSA Calculations. *International J Mol Sci*. 2012; *13*(4): 4545. https://doi.org/10.3390/ijms13044545

27. Santos JRC, Abreu PE, Marques JS. Towards nature-inspired materials for adsorbing pesticides: a multi-stage computational approach. *PCCP***.**2025; *27*(35): 18665. https://doi.org/10.1039/d5cp01445j

28. Haque MA, Lee JH, Cho KM. Endophytic bacterial diversity in Korean kimchi made of Chinese cabbage leaves and their antimicrobial activity against pathogens. *Food*

Control.2015; 56: 24-33. doi: 10.1016/j.foodcont.2015.03.006
29. Mamun MAA, Hossain MS, Debnath GC, Sultana S, Rahman A, Hasan Z, Haque MA. Unveiling lignocellulolytic trait of a goat omasum inhabitant *Klebsiella variicola* strain HSTU-AAM51 in light of biochemical and genome analyses. *Braz J Microbiol*.2022 ;53(1): 99-130. doi: 10.1007/s42770-021-00660-7
30. Haque MA, Hong SY, Hwang CE, Kim SC, Cho KM. Cloning of an organophosphorus hydrolase (opdD) gene of *Lactobacillus sakei* WCP904 isolated from chlorpyrifos-impregnated kimchi and hydrolysis activities of its gene product for organophosphorus pesticides. *Appl Biol Chem*.2018;61(6): 643-651. DOI:10.1007/s13765-018-0397-x
31. Haendiges J, Jinneman KC, González-Escalona N. Choice of library preparation affects sequence quality, genome assembly, and precise in silico prediction of virulence genes in shiga toxin-producing *Escherichia coli*. *PLoS ONE*. 2021:*16*(3). https://doi.org/10.1371/journal.pone.0242294
32. Darling AE, Mau B, Perna NT. progressiveMauve: Multiple genome alignment with gene gain, loss and rearrangement. *PLoS ONE.*2010;*5*(6). https://doi.org/10.1371/journal.pone.0011147
33. Haque MA**,** Hossain MS, Ahmad I, Akbor MA, Rahman A, Manir MS, Patel HM and Cho KM. Unveiling chlorpyrifos mineralizing and tomato plant-growth activities of *Enterobacter* sp. strain HSTU-ASh6 using biochemical tests, field experiments, genomics, and in silico analyses. *Front. Microbiol*. 2022; 13:1060554. doi: 10.3389/fmicb.2022.1060554.
34. Haque, M A, Simo, Prodhan MY, Ghosh S, Hossain MS, Rahman A, Haque MA. Enhanced rice plant (BRRI-28) growth at lower doses of urea caused by diazinon mineralizing endophytic bacterial consortia and explorations of relevant regulatory genes in a *Klebsiella* sp. strain HSTU-F2D4R. *Arch Microbiol*.2023; 205(6): 231. doi: 10.1007/s00203-023-03564-2
35. Galperin MY, Kristensen DM, Makarova KS, Wolf YI, Koonin EV. Microbial genome analysis: the COG approach. *Brief Bioinform*. 2017; *20*(4):1063.https://doi.org/10.1093/bib/bbx117
36. Larsen MV, Cosentino S, Rasmussen S, Friis C, Hasman H, Marvig RL, Jelsbak L, Sicheritz-Pontén T, Ussery DW, Aarestrup FM, Lund O. Multilocus sequence typing of total-genome-sequenced bacteria. J clin microbiol. 2012 Apr;50(4):1355-61. doi: 10.1128/JCM.06094-11
37. Kumar P. Bacilli-mediated degradation of xenobiotic compounds and heavy. Advanced bioremediation technologies and processes for the treatment of synthetic organic compounds (SOCs). *Front Bioeng Biotechnol*. 2020 ;8: 570307.doi: 10.3389/fbioe.2020.570307.
38. Lee HY, Cho DY, Ahmad I, Patel HM, Kim MJ, Jung JG, Cho KM. Mining of a novel esterase (est3S) gene from a cow rumen metagenomic library with organosphosphorus insecticides degrading capability: Catalytic insights by site directed mutations, docking, and molecular dynamic simulations.*Int J Biol Macromol. 2021 ;190: 441-455.doi: 10.1016/j.ijbiomac.2021.08.224*
39. Haque AM, Hwang CE, Kim SC, Cho DY, Lee HY, Cho KM, Lee JH. Biodegradation of organophosphorus insecticides by two organophosphorus hydrolase genes (*opd*A and *opd*E) from isolated *Leuconostoc mesenteroides* WCP307 of kimchi origin. *Process Biochem* .2020:94: 340-348. DOI: 10.1016/j.procbio.2020.04.026
40. Zhang x, Liu Y, Wang J, Zhao Y, Deng Y. Biosynthesis of adipic acid in metabolically engineered *saccharomyces cerevisiae. J microbiol*. 2020; 58(12): 1065-1075. doi: 10.1007/s12275-020-0261-7
41. Chaudhary P, Agri U, Chaudhary A, Kumar A, Kumar G. Endophytes and their potential in biotic stress management and crop production. *Front Microbiol*. 2022; *13*. https://doi.org/10.3389/fmicb.2022.933017
42. Grondin JM, Tamura K, Déjean G, Abbott DW, Brumer H. polysaccharide utilization loci: fueling microbial communities. *J Bacteriol*. 2017; *199*(15). https://doi.org/10.1128/jb.00860-16.
43. Christiansen S, Bendevis MA. Plant Biology Europe 2018 Conference: Abstract Book. *Forskerportalen* ;2018.
44. Jain C, Rodriguez-RLM, Phillippy AM, Konstantinidis KT, Aluru S. High throughput ANI analysis of 90K prokaryotic genomes reveals clear species boundaries. *Nat Commun*. 2018; *9*(1): 5114. https://doi.org/10.1038/s41467-018-07641-9
45. Rodriguez-RLM, Conrad RE, Viver, T, Feistel DJ, Lindner BG, Venter SN, Orellana LH, Amann R, Rosselló-Mora R, Konstantinidis KT. An ANI gap within bacterial species that advances the definitions of intra-species units. *mBio*. 2023; *15*(1). https://doi.org/10.1128/mbio.02696-23.
46. Hu S, Li K, Zhang Y, Wang Y, Fu L, Xiao Y, Tang X, Gao J. New insights into the threshold values of multi-locus sequence analysis, average nucleotide identity and digital DNA–DNA hybridization in delineating Streptomyces species. *Frontiers Microbiology*. 2022; 13:910277. https://doi.org/10.3389/fmicb.2022.910277
47. Valiente-Mullor C, Beamud B, Ansari I, Francés-Cuesta C, García-González N, Mejía L, Ruiz-Hueso P, González-Candelas F. One is not enough: On the effects of reference genome for the mapping and subsequent analyses of short-reads. *PLoS computational biology.*2021, *17*(1), e1008678. https://doi.org/10.1371/journal.pcbi.1008678
48. Thänert R, Choi J, Reske KA, Hink T, Thänert A, Wallace MA, Wang B, Seiler S, Cass C, Bost MH, Struttmann E, Iqbal ZH, Sax SR, Fraser VJ, Baker AW, Foy K, Williams B, Xu B, Capocci-Tolomeo P, Dantas G. Persisting uropathogenic *Escherichia coli* lineages show signatures of niche-specific within-host adaptation mediated by mobile genetic elements. *Cell Host & Microbe*. 2022;*30*(7): 1034. https://doi.org/10.1016/j.chom.2022.04.008
49. Zhao Y, Wei HM, Yuan J, Xu L, Sun JQ. A comprehensive genomic analysis provides insights on the high environmental adaptability of *Acinetobacter* strains. *Front Microbiol*. 2023; *14*: 1177951. https://doi.org/10.3389/fmicb.2023.1177951
50. Rodrigues DLN. Comparative genomics of *Acinetobacter baumannii*: pan-resistome and evolution. Federal University of Minas Gerais; 2021.

51. Urhan A, Abeel T. A comparative study of pan-genome methods for microbial organisms: Acinetobacter baumannii pan-genome reveals structural variation in antimicrobial resistance-carrying plasmids. *Microb. Genom*. 2021;*7*(11). https://doi.org/10.1099/mgen.0.000690

52. Castro-Jaimes S, Bello-López E, Velázquez-Acosta C, Volkow-Fernández P, Lozano-Zaraín P, Castillo-Ramírez S, Cevallos MA. chromosome architecture and gene content of the emergent pathogen *acinetobacter haemolyticus*. *Front Microbiol*. 2020; *11*: 926. https://doi.org/10.3389/fmicb.2020.00926

53. Azarian T, Huang IT, Hanage WP. Structure and dynamics of bacterial populations: pangenome ecology. in: Tettelin h, Medini D. (eds) The Pangenome. *Springer*.2020. https://doi.org/10.1007/978-3-030-38281-0_5

54. Zhang M, Han L, Liao C, Su W, Jiang C. Comparative genomics reveals key adaptive mechanisms in pathogen host-niche specialization. *Front Microbiol.* 2025; *16*. https://doi.org/10.3389/fmicb.2025.1543610

55. Salto I, Tejerizo GT, Wibberg D, Pühler A, Schlüter A, Pistorio M. Comparative genomic analysis of *Acinetobacter spp*. plasmids originating from clinical settings and environmental habitats. *Sci Rep*. 2018; *8*(1): 7783. https://doi.org/10.1038/s41598-018-26180-3

56. Touchon M, Cury J, Yoon EJ, Křížová L, Cerqueira G, Murphy CI, Feldgarden M, Wortman JR, Clermont D, Lambert T, Grillot-Courvalin C, Nemec A, Courvalin P, Rocha EPC. The genomic diversification of the whole *acinetobacter* genus: origins, mechanisms, and consequences. *Genome Biol. Evol*. 2014;*6*(10): 2866. https://doi.org/10.1093/gbe/evu225

57. Mindlin SZ, Maslova O, Beletsky AV, Nurmukanova V, Zong Z, Mardanov AV, Ma P. Ubiquitous conjugative mega-plasmids of *acinetobacter* species and their role in horizontal transfer of multi-drug resistance. *Front Microbiol*. 2021; *12*: 728644. https://doi.org/10.3389/fmicb.2021.728644

58. Karampatakis T, Tsergouli K, ehzadi P. Pan-genome plasticity and virulence factors: a natural treasure trove for *acinetobacter baumannii*. *Antibiotics*.2024; *13*(3): 257. https://doi.org/10.3390/antibiotics13030257

59. Bruto M, Prigent-Combaret C, Müller D, Moënne-Loccoz Y. Analysis of genes contributing to plant-beneficial functions in plant growth-promoting rhizobacteria and related Proteobacteria. *Sci Rep*.2014; *4*(1). https://doi.org/10.1038/srep06261.

60. Tariq A, Tanvir A, Barasarathi J, Alsohim AS, Mastinu A, Sayyed R, NazirA. Endophytes: key role players for sustainable agriculture: mechanisms, omics insights and future prospects. *Plant Growth Regul* (2025). https://doi.org/10.1007/s10725-025-01370-y

61. Chia XK, Hadibarata T, Kristanti RA, Jusoh MNH, Tan IS, Foo HCY. The function of microbial enzymes in breaking down soil contaminated with pesticides: a review. *Bioprocess Biosyst. Eng*. 2024;*47*(5): 597. https://doi.org/10.1007/s00449-024-02978-6

62. Mali H, Shah C, Raghunandan BH, Prajapati AS, Patel D, Trivedi U, Subramanian R. Organophosphate pesticides an emerging environmental contaminant: Pollution, toxicity, bioremediation progress, and remaining challenges. *Environ. Sci.* 2022; *127*: 234. https://doi.org/10.1016/j.jes.2022.04.023

63. Thakur M, Medintz IL, Walper SA. Enzymatic bioremediation of organophosphate compounds-progress and remaining challenges. *Front. Bioeng. Biotechnol.* 2019; *7*. https://doi.org/10.3389/fbioe.2019.00289

64. Ganie SA, Bhat JA, Devoto A. The influence of endophytes on rice fitness under environmental stresses. *Plant Mol. Biol.* 2021; *109*: 447. https://doi.org/10.1007/s11103-021-01219-8

65. Khoury LE, Mobley DL, Ye D, Rempe SB. Enhancing paraoxon binding to organophosphorus hydrolase active site. *Int J Mol Sci*. 2021; *22*(23): 12624. https://doi.org/10.3390/ijms222312624

66. Jin H, Zhou Z, Wang D, Guan S, Han W. Molecular dynamics simulations of acylpeptide hydrolase bound to chlorpyrifosmethyl oxon and dichlorvos. *Int J Mol Sci*. 2015;*16*(3): 6217. https://doi.org/10.3390/ijms16036217

67. Bigley AN, Raushel FM. Catalytic mechanisms for phosphotriesterases. *Biochim Biophys Acta.* 2013 ;1834(1):443-53. doi: 10.1016/j.bbapap.2012.04.004.

68. Ramalho TC, Castro AA, Silva DR, Silva MC, França TCC, Bennion BJ, Kuča K. Computational enzymology and organophosphorus degrading enzymes: promising approaches toward remediation technologies of warfare agents and pesticides. *Curr. Med. Chem*. 2016; *23*(10): 1041. https://doi.org/10.2174/0929867323666160222113504

69. Xu W, Zhao S, Zhang W, Wu H, Guang C, Mu W. Recent advances and future prospective of organophosphorus-degrading enzymes: identification, modification, and application. *Crit Rev Biotechnol* 2021; *41*(7): 1096. https://doi.org/10.1080/07388551.2021.1898331

70. Nagrale T, Chaurasia A, Kumar S, Gawande SP, Hiremani NS, Shankar R, Gokte-Narkhedkar N, Renu R, Prasad Y G. PGPR: the treasure of multifarious beneficial microorganisms for nutrient mobilization, pest biocontrol and plant growth promotion in field crops. *World J. Microbiol. Biotechnol*. 2023; *39*(4): 100. https://doi.org/10.1007/s11274-023-03536-0

71. Giri BS, Geed SR, Vikrant K, Lee SS, Kim K, Kailasa SK, Vithanage M, Chaturvedi P, Nath B, Singh RS. Progress in bioremediation of pesticide residues in the environment. *Environ. Eng. Res*. 2020; *26*(6): 200446. https://doi.org/10.4491/eer.2020.446.